# Timing and magnitude of depth-dependent lithosphere stretching on the southern Lofoten and northern Vøring continental margins offshore mid-Norway: implications for subsidence and hydrocarbon maturation at volcanic rifted margins

N. J. KUSZNIR,[1] R. HUNSDALE[2], A. M. ROBERTS[3] and iSIMM Team[4]

[1]*Department of Earth Sciences, University of Liverpool, Liverpool L69 3BX, UK (e-mail: n.kusznir@liverpool.ac.uk)*
[2]*ConocoPhillips, P.O. Box 220, 4098 Tananger, Norway (current address, Statoil, 4035 Stavanger, Norway)*
[3]*Badley Geoscience, Hundleby, Spilsby, Lincolnshire PE23 5NB, UK*
[4]*iSIMM Team comprises P. A. F. Christie, N. J. Kusznir, A. M. Roberts, R. S. White, N. W. Hurst, V. Tymms, D. Healy, Z. C. Lunnon, C. J. Parkin, A. W. Roberts, L. K. Smith & R. Spitzer*

**Abstract:** Subsidence analysis on the southern Lofoten and northern Vøring segments of the Norwegian rifted margin shows depth-dependent stretching of continental margin lithosphere in which lithosphere stretching and thinning at continental break-up at ~54 Ma greatly exceeds that of the upper crust within 100 km landward of the COB. For the southern Lofoten margin lithosphere β stretching factors approaching infinity are required at 54 Ma west of the Utrøst Ridge to restore the top Basalt (inner lava flow) reflectors and top Tare formation (54 Ma) to presumed sub-aerial depositional environments, while for the northern Vøring margin lithosphere β values of 2.5 are required. In contrast, upper crustal extension by faulting shows little stretching with $\beta < 1.1$ at break-up or immediately preceding break-up in the Paleocene and Late Cretaceous. The presence of lithosphere depth-dependent stretching and the absence of significant Paleocene and Late Cretaceous upper crustal extension imply that depth-dependent stretching of the southern Lofoten and northern Vøring margins occurred during sea-floor spreading initiation rather than during pre-break-up intra-continental rifting. Depth-dependent stretching, where upper-crustal extension is significantly smaller than whole-crustal or whole-lithosphere extension within 75–150 km of the COB, has been observed worldwide for both volcanic and non-volcanic rifted continental margins. Temperature and hydrocarbon maturation modelling show that the inclusion of depth-dependent stretching has an important effect on temperature and hydrocarbon maturation evolution in depth and time. Failure to include the large β factors for the lower crust and lithospheric mantle (below the less stretched upper crust) leads to a serious under-prediction of temperature and hydrocarbon maturation. While the effect of emplacing thick sill intrusions or magmatic underplating at continental break-up has an important effect on predicted temperature and %VR, their effects can be small in comparison with that of depth-dependent stretching.

**Keywords:** rifted continental margins, continental break-up, continental rifting, depth-dependent lithosphere stretching, heat flow, hydrocarbon maturation, Norwegian continental margin

Depth-dependent lithosphere stretching, in which extension and thinning of the whole crust and lithosphere of the rifted continental margin greatly exceeds that of the upper crust, has been observed at many rifted continental margins (Roberts *et al*. 1997; Driscoll & Karner 1998; Davis & Kusznir 2004). Stretching estimates may be independently determined for the upper crust, the whole crust, and the lithosphere for continental rifted margins using three independent data sets and methodologies (Fig. 1a). Extension and thinning of the upper crust may be measured using fault heaves from seismic reflection data; of the whole crust using crustal basement thinning derived from crustal structure using wide angle seismology and gravity studies; and of the whole lithosphere from post-break-up subsidence using flexural backstripping of post-break-up stratigraphic data.

An example of these three independent stretching and thinning estimates is shown for the Goban Spur rifted margin in Figure 1b–d. Profiles of β stretching factors and thinning factor (1-1/β) show upper crustal stretching and thinning which is substantially less than that of the whole crust and lithosphere within approximately 100 km landward of the continent–ocean boundary. Error analysis shows that the stretching and thinning differences between the upper crust, and the deeper whole crust and lithosphere levels are statistically significant for this region (Davis & Kusznir 2004). Further towards the continent, stretching and thinning estimates converge as β factors tend to 1. Similar analyses have been carried out for the South China Sea, Galicia, Vøring, Møre, Vulcan and Exmouth Plateau margins (Roberts *et al*. 1997; Driscoll & Karner 1998; Baxter *et al*. 1999; Davis & Kusznir 2004) and show similar results in which stretching of the whole crust and lithosphere of continental margins greatly exceeds that of the upper crust. The total margin extension may be determined by integrating the thinning-factor (1-1/β) across the continental margin. Margin extension is summarized in Figure 1e for a number of rifted continental margins. In all cases stretching of the whole crust and lithosphere exceeds that of the upper crust. Depth-dependent stretching is observed at both non-volcanic and volcanic continental margins.

A key question is the timing of depth-dependent lithosphere stretching at rifted margins. Does depth-dependent stretching occur during pre-breakup intracontinental rifting, or does depth-dependent stretching occur during sea-floor spreading initiation? In order to answer this question, good stratigraphic resolution of the pre- and post-break-up stages

KUSZNIR, N. J., HUNSDALE, R., ROBERTS, A. M. & iSIMM Team 2005. Norwegian margin depth-dependent stretching. *In*: DORÉ, A. G. & VINING, B. A. (eds) *Petroleum Geology: North-West Europe and Global Perspectives—Proceedings of the 6th Petroleum Geology Conference*, 767–783. 

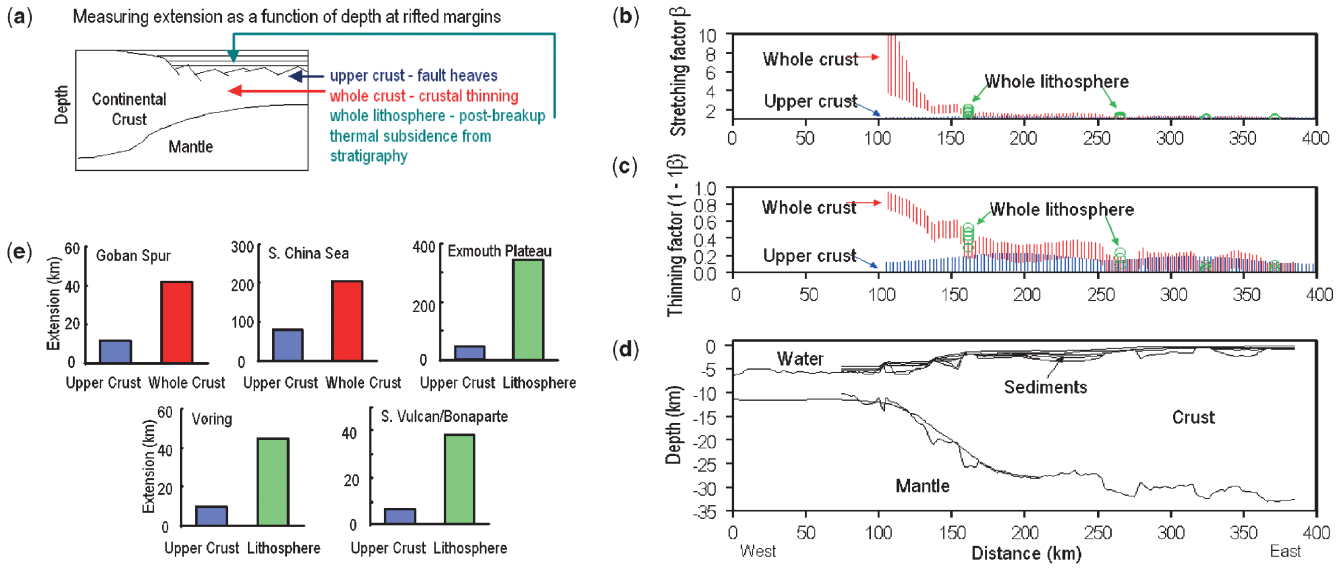


**Fig. 1.** (**a**) Continental margin extension and thinning can be measured at the levels of the upper crust, the whole crust and the lithosphere using three distinct data sets and techniques. (**b**–**d**) Example of depth-dependent stretching for the Goban Spur non-volcanic margin. Stretching of the upper crust is much less than that of the whole crust and lithosphere. (**e**) Comparison of upper crustal, whole crustal and lithosphere extension showing depth-dependent stretching for the Goban Spur, S. China Sea, Exmouth Plateau, Vøring and Vulcan Basin margins.

of margin evolution is required. The Lofoten and Vøring rifted margins have good stratigraphic resolution of the Upper Cretaceous and Paleocene sequences preceding continental break-up and sea-floor spreading initiation at ~54 Ma.

An analysis of pre- and post-break-up subsidence, and Paleocene and Late Cretaceous upper-crustal fault extension has been carried out on the southern Lofoten and northern Vøring margins. Three profiles have been studied and their locations are shown in Figure 2a on a map showing the N Atlantic pre-break-up margin restoration at ~54 Ma (adapted from Eide, 2002) and in Figure 2b showing the present-day margin geometry and continent ocean boundary (adapted from Tsikalas *et al.* 2001). The three profiles form part of a regional study on the mid-Norway Margin involving the construction of regional cross sections extending from the area of the continent–ocean boundary to close to the coast. Horizon picking from seismic reflection data was constrained by well data where possible. The sections were depth converted using a regional velocity model that incorporated all available well information and seismic stacking velocities. The depth sections also satisfactorily model the present-day gravity field. Pre-basalt sediment thickness and basalt thicknesses were determined using seismic refraction and potential field data (Mjelde *et al.* 1993; Tsikalas *et al.* 2001). Geological interpretations of depth converted seismic sections for the three profiles are shown in Figure 2c–e. Profile 3 extends westwards on to oceanic crust according to magnetic anomaly data and other geophysical work (Mjelde *et al.* 1993; Tsikalas *et al.* 2001, 2002; Mosar *et al.* 2002; Sigmond, 2002), while profiles 1 and 2 extend westwards to near the continent–ocean boundary. Profile 2 crosses the Bivrost Lineament.

The Lofoten and Vøring margins, like most of the NW European continental margin, have a prolonged history of extension from the Devonian through to continental break-up at the start of the Eocene (Eldholm *et al.* 1989; Doré, 1991; Blystad *et al.* 1995; Skogseid & Eldholm *et al.* 2000; Lundin & Doré, 1997; Doré *et al.* 1999; Roberts *et al.* 1999; Brekke 2000). The main rift phases are widely held to be Early Triassic, Middle to Late Jurassic, Early Cretaceous, and Late Cretaceous to Paleocene leading to break-up at the beginning of the Eocene (Talwani & Eldholm 1977; Eldholm *et al.* 1989; Blystad *et al.* 1995; Skogseid *et al.* 2000; Lundin & Doré, 1997). The Norwegian–Greenland Sea opened during Chron 24r (53.35–55.90 Ma: Cande & Kent, 1992; Talwani & Eldholm 1977; Skogseid *et al.* 2000; Tsikalas *et al.* 2002). The age of break-up is estimated from the age of the first definitive magnetic anomaly, Anomaly 24B (Sigmond, 2002; Skogseid *et al.* 2000; Tsikalas *et al.* 2002) which, based on the timescale of Cande & Kent (1992), has an age of 53.9 Ma and lies within the earliest Eocene. Tsikalas *et al.* (2002) have suggested that early opening may have commenced at ~54.6 Ma. For modelling purposes we use 54 Ma for the age of the top Tare Formation reflector (Dalland *et al.* 1988; Berggren *et al.* 1995; Ren *et al.* 2003) and 54.1 Ma for the age of break-up and top Basalt inner lava flow reflector. The break-up of the Norwegian continental margin took place in the presence of a mantle plume or mantle hot spot, leading to the formation of a volcanic margin (White & McKenzie 1989, 1995; Eldholm *et al.* 1995).

The analysis of pre- and post-break-up subsidence has been carried out using reverse post-rift subsidence modelling, consisting of flexural backstripping and reverse post-break-up thermal subsidence modelling. The principles of this technique are summarized in Figure 3a and are described in detail in Kusznir *et al.* (1995) and Roberts *et al.* (1998). Using this analysis technique, a present-day depth-converted section is sequentially backstripped to base post-rift or base post-break-up, the remaining stratigraphic units are decompacted, and the flexural isostatic rebound due to sediment load removal and decompaction is computed and applied to the backstripped and decompacted section. In addition post-rift or post-break-up thermal subsidence is applied to the backstripped section using flexural isostasy.

**Fig. 2.** The location of lines 1, 2 and 3 on the southern Lofoten and northern Vøring margins used in this study superimposed on (**a**) plate reconstruction to ~54 Ma (after Eide, 2002) and (**b**) present-day map showing ocean isochrons, COB and main structural elements (after Tsikalas *et al.* 2001). Line 2 and 3 are located on the southern Lofoten margin. Line 1 is located on the northern Vøring margin. Line 3 extends 50 km onto oceanic crust to the NW (Mosar *et al.* 2002). Line 2 crosses the Bivrøst Lineament. (**c**–**e**) Interpretations of depth converted cross sections for Lines 1, 2 and 3. UR, Utrøst Ridge; COB, continent–ocean boundary; BFZ, Bivrøst Fracture Zone; JMFZ, Jan Mayen Fracture Zone.

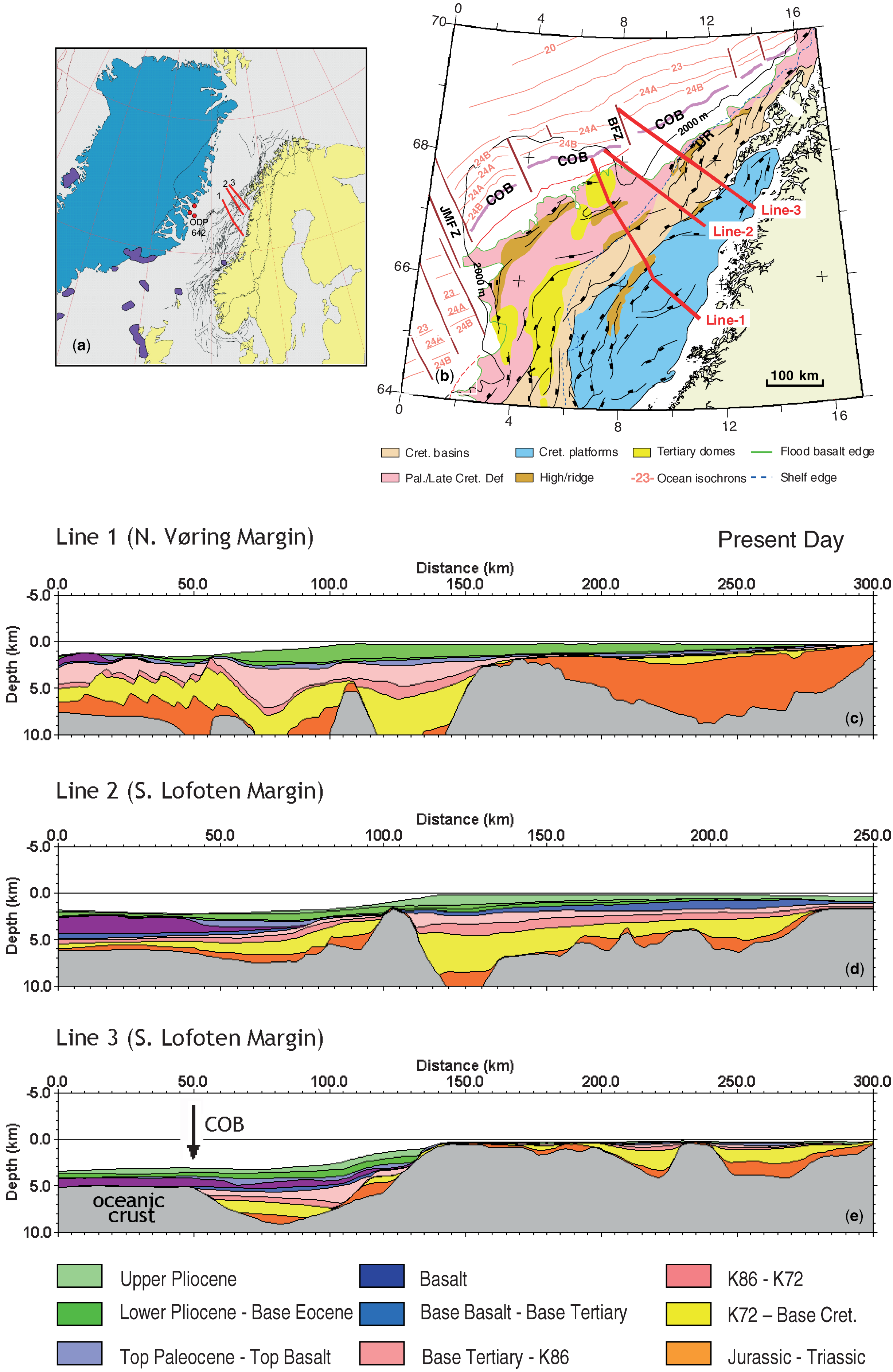
(a)
ODP 642
1
2 3
(b)
COB
BFZ
JMFZ
2000 m
Line-1
Line-2
Line-3
100 km
Cret. basins
Pal./Late Cret. Def
Cret. platforms
High/ridge
Tertiary domes
-23- Ocean isochrons
Flood basalt edge
Shelf edge
Line 1 (N. Vøring Margin)
Present Day
Distance (km)
Depth (km)
(c)
Line 2 (S. Lofoten Margin)
(d)
Line 3 (S. Lofoten Margin)
COB
oceanic crust
(e)
Upper Pliocene
Lower Pliocene - Base Eocene
Top Paleocene - Top Basalt
Basalt
Base Basalt - Base Tertiary
Base Tertiary - K86
K86 - K72
K72 – Base Cret.
Jurassic - Triassic

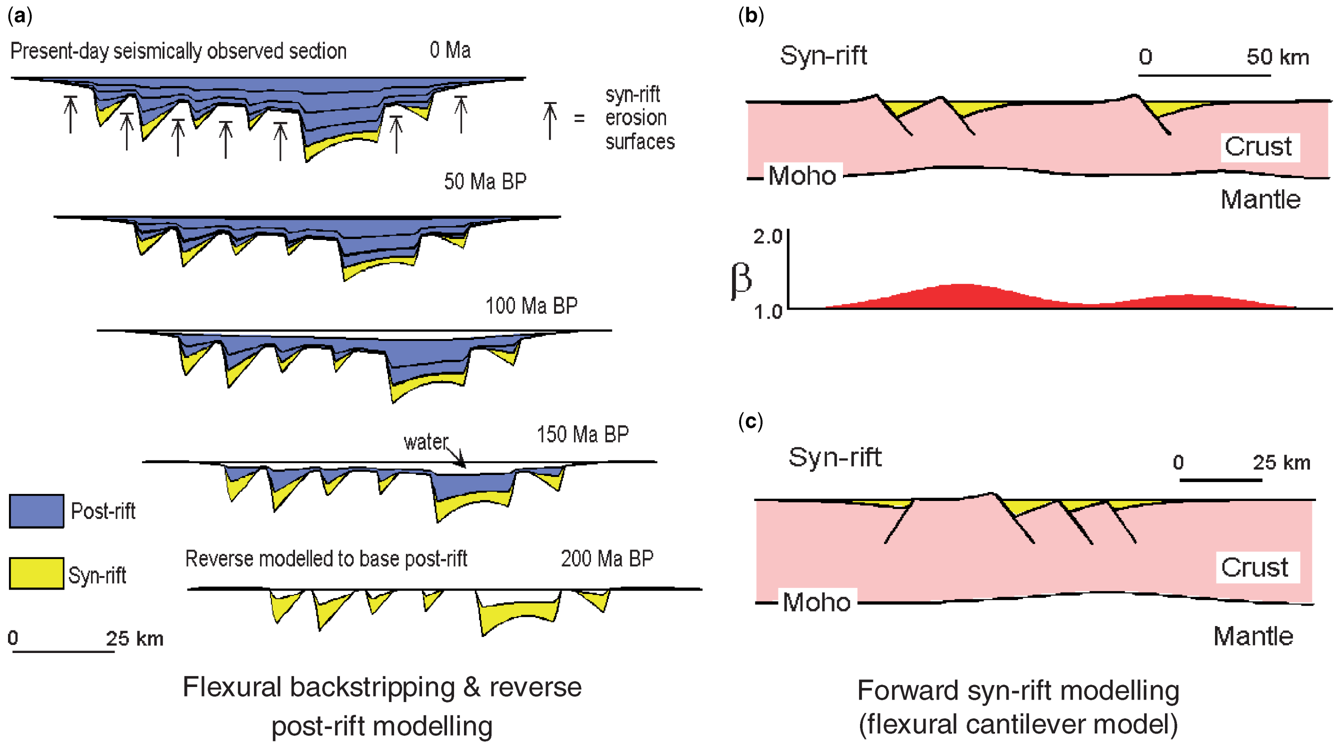


**Fig. 3.** (**a**) Schematic diagram showing application of flexural backstripping and reverse post-rift modelling to predict sequential restorations of post-rift stratigraphy and palaeobathymetry. Restored sections are dependent on the β factor used to define the magnitude of lithosphere extension at rifting and lithosphere flexural strength during isostatic load removal. Flexural backstripping and reverse post-rift modelling may be used to determine the β factor from a knowledge of palaeobathymetry. (**b**) Schematic diagrams showing application of the flexural cantilever model of continental lithosphere extension to the syn-rift stage of basin development. Crustal extension of the upper crust on planar faults generates footwall uplift and hanging wall collapse. Plastic deformation in the lower crust and mantle are quantified by a 2D β stretching-factor. (**c**) The interference of footwall uplift and hanging-wall collapse gives rise to the familiar half-grabens, rotated fault blocks and horsts of rift tectonics depending on fault polarity.

Post-break-up thermal subsidence depends on lithosphere stretching and is computed using a trial β factor (McKenzie 1978). The application of flexural backstripping and reverse post-break-up thermal modelling produces a series of restored sections, which can be tested or calibrated against observed palaeobathymetry data. This technique may be used to predict palaeobathymetry from known β factor distribution, or alternatively (as in the case of the work described in this paper) can be used to determine β factor distribution from palaeobathymetry constraints. The analysis of Paleocene and Late Cretaceous upper-crustal fault extension has been carried out using the flexural cantilever model of continental lithosphere extension. This technique may be used to forward model syn- and post-rift basin development (Fig. 3b and c), and is described in detail in Kusznir *et al.* (1991) and Kusznir & Ziegler (1992). The flexural cantilever model has been used to quantify lithosphere extension associated with faulting during the Paleocene and Late Cretaceous. Whole crustal thinning and stretching have not been determined for the Lofoten Margin because volcanic addition has also modified crustal thickness (Mjelde *et al.* 1993).

A key requirement of our subsidence analysis using reverse post-rift subsidence modelling is knowledge of the palaeobathymetries of the top Tare and top Basalt reflector levels in order to determine the lithosphere β factors controlling post-break-up thermal subsidence. ODP and DSDP well data suggest that the Tare formation and basalt inner flow sequences were deposited or extruded in a terrestrial or shallow marine environment (Eldholm *et al.* 1989), or that basaltic and sediment material of this age were emergent and being eroded (Caston 1976; Talwani & Eldholm 1972). A more comprehensive discussion of palaeobathymetry, depositional environments and age constraints at break-up on thesouthern Lofoten and northern Vøring margins is given in Kusznir *et al.* (2004).

## Depth-dependent stretching on the southern Lofoten and northern Vøring margins

The analysis of pre- and post-break-up subsidence and faulting of the three Lofoten and Vøring margin profiles was carried out as part of a regional study designed to develop a tectono-stratigraphic framework for the Norwegian Sea. Particular aims of the study were the evaluation of the tectonic history of the Lofoten Margin through structural and stratigraphic modelling, and on the determination of the spatial and temporal distribution of lithosphere subsidence and stretching.

### *Line 2 (southern Lofoten Margin)*

*Break-up rifting.* Flexural backstripping and reverse post-break-up modelling has been carried out for the three modelled cross sections to determine the break-up lithosphere β factor. The preferred model of the present-day section for line 2, restored to top Tare formation and top Basalt times, is shown in Figure 4. This modelling procedure restores top Tare and top Basalt to near sea-level at ~54 Ma (break-up age) consistent with their palaeobathymetries at that time. The preferred restoration requires a break-up lithosphere β stretching factor, which approaches infinity towards the ocean and rapidly tends to β = 1 east of the Utrøst Ridge.

An earlier rift event with β = 1.3 at 142 Ma is included in the model to represent the residual thermal subsidence of the earlier Late Jurassic–Early Cretaceous rift event (Roberts *et al.* 1997). The omission of the earlier Late Jurassic–Early Cretaceous rift event in the flexural backstripping and reverse post-break-up modelling would lead to an increase in the magnitude of the break-up lithosphere β factors required to restore top Tare and top Basalt to near sea-level at ~54 Ma. Sensitivity tests of the determined

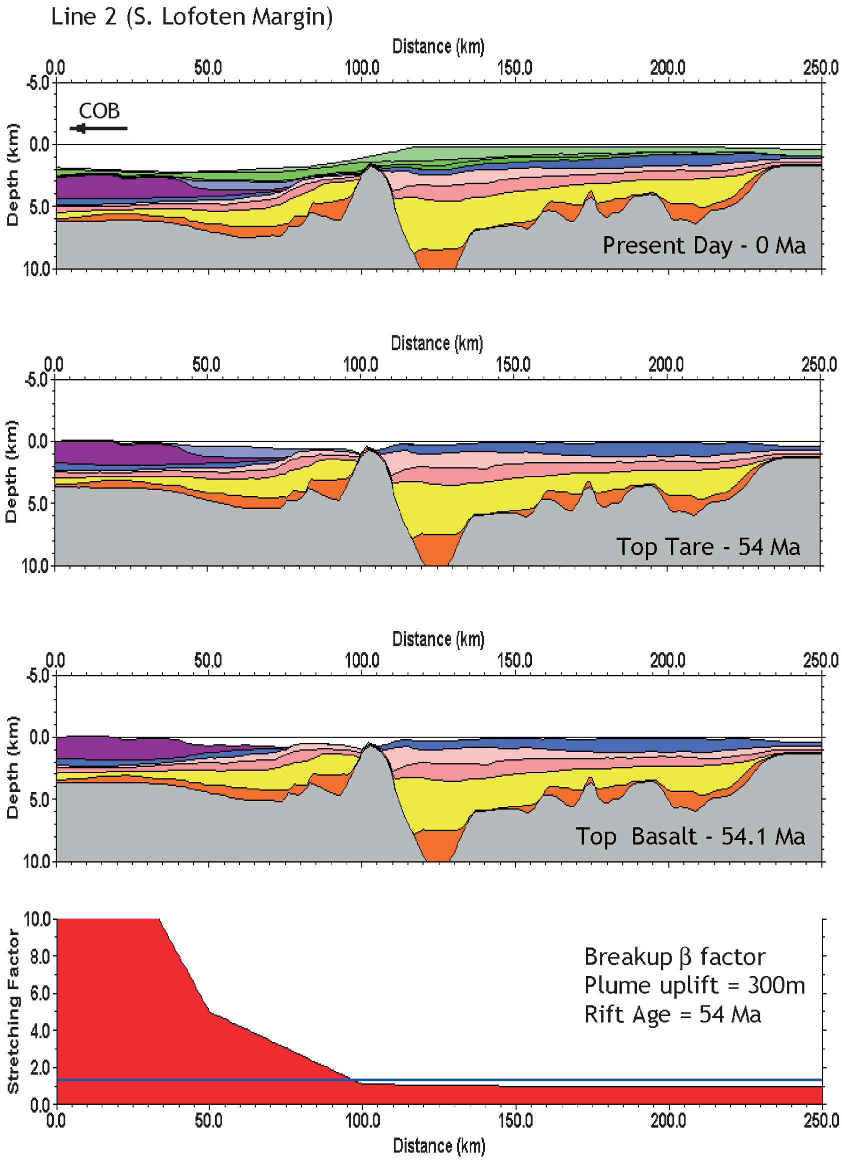


**Fig. 4.** Restored cross sections for line 2 (southern Lofoten margin) produced by 2D flexural backstripping and reverse post-rift modelling from present day to top Tare at 54 Ma and top Basalt reflector levels at 54.1 Ma. Break-up age is 54.1 Ma. Lithosphere β factor varies laterally decreasing from β = infinity near COB in the west to β = 1 in east. Transient mantle plume uplift for Upper Paleocene is 300 m. Earlier Jurassic-Cretaceous rift at 142 Ma with β = 1.3. Lithosphere effective elastic thickness $T_e$ = 3 km. The top Tare and top Basalt horizons are restored to sea-level at ~54 Ma consistent with depositional environments.

break-up lithosphere β factor to the magnitude of Late Jurassic–Early Cretaceous rifting is given by Roberts *et al*. (1997). Volcanic addition through sill intrusion and magmatic underplating undoubtedly occurred during the Paleocene prior to continental break-up at ~54 Ma. The flexural backstripping and reverse post-break-up modelling procedure shown in Figure 4 restores a present-day section to top Tare and top Basalt time at ~54 Ma. Any permanent crustal uplift due to magmatic underplating occurring before break-up will not effect the restoration shown in Figure 4. If permanent uplift due to magmatic underplating did take place since break-up at ~54 Ma, this would lead to an underestimate of break-up lithosphere stretching-factors.

Restored cross sections using constant β factors of 1, 2, 5 and infinity to define the reverse thermal subsidence are shown in Figure 5. Increasing the break-up β factor to significantly greater than β = 1 east of the Utrøst Ridge produces a restoration of top Tare and top Basalt reflectors at ~54 Ma too high above sea-level which is inconsistent with palaeobathymetric evidence, while using values of β factor significantly less than infinity on the western oceanic end of the profile fails to restore top Tare and top Basalt reflectors to sea-level at ~54 Ma.

The preferred restoration model (Fig. 4) includes a Late Paleocene plume dynamic uplift with amplitude of 300 m (Nadin & Kusznir 1995; Nadin *et al.* 1997). While the large lithosphere β factors at the oceanic end of the profile may be reduced by increasing plume dynamic uplift above 300 m, larger values of Paleocene plume uplift elevate the continental part of the section east of the Utrøst Ridge too high at top Tare and top Basalt times, leading to erosion which is not observed. The preferred restoration model uses a lithosphere elastic thickness ($T_e$) of 3 km. Tests show that the restorations and the derived break-up lithosphere β factor are not sensitive to $T_e$ due to the relatively long wavelength of the sediment and thermal subsidence loads. Sensitivity tests to β factor $T_e$ and rift age are shown in greater detail in Kusznir *et al.* (2004).

*Paleocene rifting*. The results of flexurally backstripping, decompaction and reverse thermal subsidence modelling of the line 2 section from top Tare to base Tertiary at 65 Ma are shown in

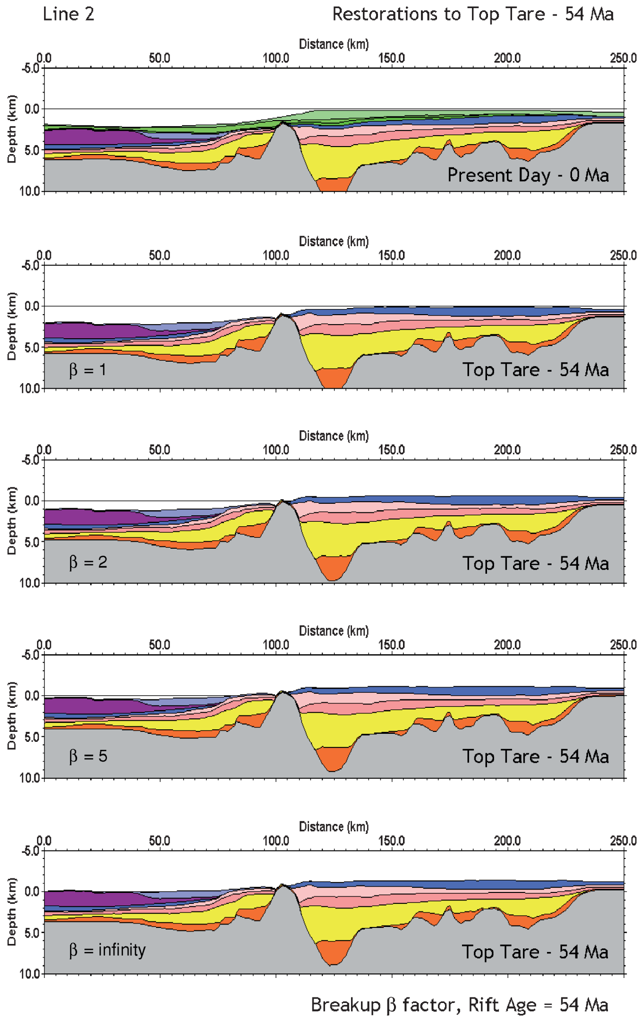


**Fig. 5.** Sensitivity tests of restored cross sections for line 2 (southern Lofoten margin) to lithosphere β factors. Restored cross section are shown for constant β factors of 1, 2, 5 and infinity and correspond to top Tare time (54 Ma). Break-up age is 54 Ma. A lithosphere β factor of infinity is required in the west of the profile to restore top Tare to sea level at 54 Ma. Lithosphere β factors of 1 are required in the east of the section in order to avoid elevating the eastern part of the section above level. Other modelling parameters are identical to those of the model shown in Figure 4.

Figure 6. The starting point for this restoration sequence is a section backstripped, decompacted and flattened to sea-level at top Tare, consistent with the near sea-level palaeobathymetries thought to exist at this time. The preferred restoration uses β = 1 for Paleocene rifting, and an earlier rift event with β = 1.3 at 142 Ma. Using a Paleocene stretching-factor significantly greater than β = 1 produces a set of Paleocene restorations that become increasingly emergent as time is wound back to 65 Ma, which is inconsistent with the observed depositional environments. The restorations from top Tare to 65 Ma (Fig. 6) show that no significant Paleocene faulting occurred prior to break-up and that the associated Paleocene lithosphere stretching factor is negligible.

*Late Cretaceous rifting.* Late Cretaceous faulting and lithosphere extension has been investigated for line 2 by backstripping and reverse thermal subsidence modelling the section from 65 Ma to 81.5 Ma, from a starting section obtained by backstripping, decompaction and flattening to sea-level at 65 Ma, consistent with the near sea-level palaeobathymetries thought to exist at this time. The Late Cretaceous sections produced by reverse modelling are shown in Figure 7, and use a Late Cretaceous β factor of 1.05 (at 81.5 Ma) and an earlier Late Jurassic–Early Cretaceous rift β factor of 1.3 (at 142 Ma). The restored sections in the interval 65 to 81.5 Ma show very little evidence of faulting other than a large eastward dipping fault to the east of the Utrøst Ridge, and smaller westward dipping faults to the west of the Utrøst Ridge. The use of a Late Cretaceous β factor much greater than 1.05 in the reverse thermal subsidence model elevates the restored section too high above sea-level at 81.5 Ma, inconsistent with the marine depositional environments thought to have existed during the Late Cretaceous on the Lofoten margin.

Late Cretaceous extensional faulting on line 2 has also been forward modelled using the flexural cantilever model (Fig. 3). This technique has been used to quantify the upper-crustal fault extension during this time. The reverse modelled section to 81.5 Ma (Fig. 7) has been used as a target to constrain the forward model. The forward model (Fig. 7) gives a peak β factor of 1.03 for Late Cretaceous extension on line 2. The combined techniques of reverse post-rift modelling and forward flexural cantilever modelling give an upper bound of β = 1.05 for Late Cretaceous extension on line 2.

Additional mid-Cretaceous continental rifting of Aptian-Albian age also occurred on the Lofoten and northern Vøring margin. However lithosphere extension at this time was small in comparison to that of break-up at ~54 Ma and is beyond the scope of this paper.

## *Line 1 (northern Vøring Margin)*

*Break-up rifting.* This profile is located in the northern part of the Vøring Basin to the south of the Bivrost Fracture Zone and Lineament. Reverse post-break-up modelling of line 1 (Fig. 8), using a similar approach to that used for line 2, predicts a break-up lithosphere β factor, decreasing from 2.5 in the west to 1 in the east, in order to restore top Tare and top Basalt to sea-level at break-up time. Break-up lithosphere β factors are substantially less than for line 2 and 3. The break-up lithosphere β factors determined from this analysis are similar to those obtained by Roberts *et al.* (1997) for the Vøring margin.

*Paleocene and Late Cretaceous rifting.* Forward and reverse modelling procedures similar to those used for line 2 have been used to investigate Paleocene and Late Cretaceous rifting for line 1 (Fig. 9). Lofoten line 1 shows a maximum β of 1.1 for Late Cretaceous rifting. This is more Late Cretaceous extension than for line 2, but very small compared with the lithosphere β stretching factor of 2.5 determined from post break-up thermal subsidence (Fig. 8). The backstripping analysis (Fig. 9) also suggests that very little extension occurred in the Paleocene compared with the Late Cretaceous.

## *Line 3 (Southern Lofoten Margin)*

*Break-up rifting.* Line 3 lies to the north of the Bivrost Fracture Zone and Lineament (Fig. 2) and extends in the west onto oceanic crust. The continent–ocean boundary is located at approximately 50 km from the western end of profile. Restored cross sections to top Tare produced by flexural backstripping and reverse thermal subsidence modelling using constant β factors of 1, 2, 5 and infinity are shown in Figure 10. Increasing the break-up β factor to significantly greater than 1 to the east of the Utrøst Ridge ($x$ = 150 km) produces a restoration of top Tare at 54 Ma too high above sea-level, which is inconsistent with palaeobathymetric evidence. For this profile, in contrast to line 2, a break-up lithosphere β factor of infinity cannot restore top Tare and top Basalt to sea-level at ~54 Ma in the west of the section. Using a break-up lithosphere β factor of infinity still produces a residual water depth of, 1500 m. The restoration models include an earlier rift event with β = 1.3 at 142 Ma to represent the earlier Late Jurassic–Early Cretaceous rift. The western 50 km of line 3 are located on oceanic crust for which the lithosphere β factor is infinity.

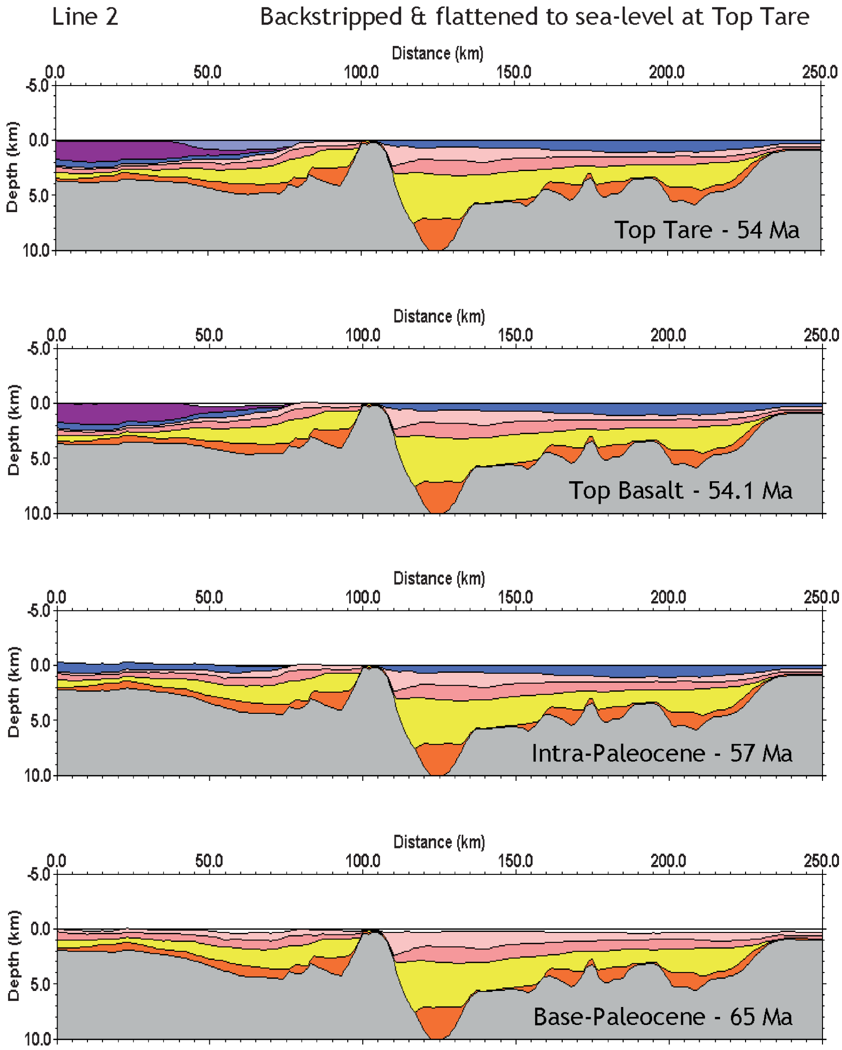


**Fig. 6.** Restored cross sections for line 2 (southern Lofoten margin) from 54 to 65 Ma produced by flexural backstripping and reverse post-rift modelling from section flattened to sea-level at 54 Ma. $\beta = 1$ (no stretching) for Early–Mid-Paleocene rift. Earlier Jurassic–Cretaceous rift at 142 Ma with $\beta = 1.3$. Transient mantle plume uplift for Upper Paleocene is 300 m. $T_e = 3$ km. The restored sections show no significant faulting in the interval 54 to 65 Ma.

The results of reverse post-break-up modelling the present-day section for line 3 to top Tare and top Basalt times at ~54 Ma, with a β factor varying from infinity for the oceanic crust in the west to $\beta = 1$ to the east of the Utrøst Ridge, are shown in Figure 11. The Paleocene plume dynamic uplift in the restorations shown in Figures 10 and 11 is 300 m (Nadin *et al*. 1997). The bathymetric discrepancy in the west can be reduced to zero by increasing the Paleocene dynamic uplift to 1500 m. However, such large plume uplift would have elevated the inboard part of the Lofoten margin high above sea-level, leading to widespread erosion, which is not observed.

The palaeobathymetries predicted for line 3 for the oceanic crust west of 50 km at top Tare (break-up) time are in the order of, 1500 m (Figs 10 and 11). This predicted oceanic palaeobathymetry is less than the water depth expected for an ocean ridge with average ocean crustal thickness but is consistent with an ocean ridge water depth where the basaltic ocean crust is overthickened, as is expected for a volcanic margin.

If the palaeobathymetric evidence for zero bathymetry at top Tare and top Basalt times, seen in the ODP and DSDP wells to the south (Caston, 1976; Talwani & Eldholm 1972; Eldholm *et al*. 1989), can be extrapolated to line 3 on the southern Lofoten margin, then the restorations shown in Figures 10 and 11 imply that line 3 experienced an additional subsidence event younger than top Tare (i.e. post-54 Ma) for the region between profile distances of 50 and 130 km. Seismic facies analysis for line 3 independently suggests that the lava sequences were emergent at the time of their deposition. If the assumption of zero bathymetry for line 3 at top Tare and top Basalt time is valid, this discrepant bathymetry and additional post-break-up subsidence had a long wavelength (>50 km), and as a consequence it is unlikely to be solely explained by hanging-wall subsidence of the major extensional fault system to the west of the Utrøst Ridge. It is more likely that this long-wavelength discrepant subsidence was generated by post-break-up Eocene thinning of the lower crust of the continental margin. This additional subsidence event may have occurred in the early Eocene during seafloor spreading initiation, although there is no available data to constrain its precise timing. An alternative mechanism for explaining the discrepant Eocene subsidence is the evacuation of molten crustal underplating material oceanward as sea-floor spreading commenced. However, lower crustal magmatic underplating bodies (LCBs) are not observed on the Lofoten continental margin segment (Mjelde *et al*. 1993, 1998; Tsikalas *et al*. 2001).

Alternatively it may be that the palaeobathymetric evidence for zero bathymetry at top Tare and top Basalt times seen in the ODP and DSDP wells to the south may not be extrapolated to line 3, and that palaeobathymetries between distances of 50 and 130 km on line 3 were in the order of, 1000 to, 1500 m, as shown in Figure 11. Planke *et al*. (2000) and Berndt *et al*. (2001) have presented evidence based on volcanic seismic facies data for a marine volcanic extrusion environment at break-up time for the Lofoten margin.

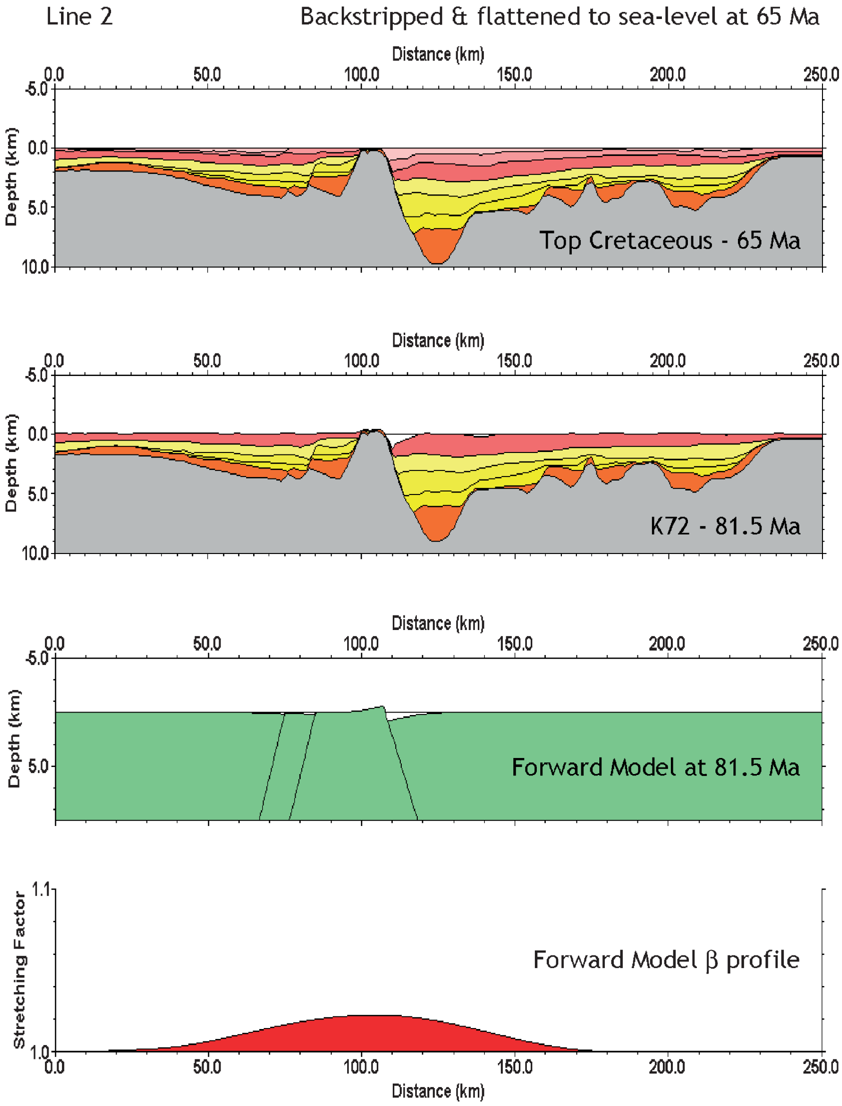


**Fig. 7.** (**a**) Restored cross sections for line 2 (southern Lofoten margin) from 65 to 81.5 Ma produced by flexural backstripping and reverse post-rift modelling from flattened section to sea-level at 65 Ma. $\beta = 1.05$ for Upper Cretaceous rift with rift age = 81.5 Ma. Earlier Jurassic–Cretaceous rift at 142 Ma with $\beta = 1.3$. Te = 3 km. The restored cross section at 81.5 Ma shows evidence of minor faulting in the interval 65 to 81.5 Ma. (**b**) 2D syn-rift forward model of Late Cretaceous rifting for southern Lofoten line 1. Target stratigraphy derived by reverse post-rift modelling to 81.5 Ma. $T_e = 3$ km. The forward model predicts a maximum β factor of 1.05. Reverse and forward models are consistent at 81.5 Ma.

### *Summary of observations for the southern Lofoten and northern Vøring margins*

For the southern Lofoten and northern Vøring margins, large β factors are required at ~54 Ma to restore top Basalt and the top Tare to sub-aerial depositional environments. In contrast these margins show upper-crustal faulting in the Paleocene and Late Cretaceous with β factors less than 1.1.The southern Lofoten and northern Vøring segments of the Norwegian margin show depth-dependent stretching of lithosphere at continental break-up. Break-up on the southern Lofoten and northern Vøring margins is not preceded by significant Paleocene or latest Cretaceous extension. The lack of significant Paleocene extension on the southern Lofoten and northern Vøring margins implies that depth-dependent stretching of the continental margin lithosphere occurred during sea-floor spreading initiation rather than pre-break-up intra-continental rifting. Depth-dependent stretching also been observed and mapped further south on the Vøring margin (Roberts *et al.* 1997) and on the Møre margin (Roberts & Hunsdale unpublished).

Depth-dependent stretching of continental margin lithosphere occurs at both volcanic and non-volcanic margins (Roberts *et al.* 1997; Driscoll & Karner 1998; Davis & Kusznir 2004). Common to all observations is stretching of the upper crust, as indicated by extensional faulting, which is substantially less than stretching and thinning of the whole crust and mantle. Possible explanations for this observation are: subseismic resolution faulting; second generation faulting; aseismic extension; and poor seismic imaging. These possible explanations are examined in detail by Davis & Kusznir (2004) who conclude that the observed extension discrepancies are real and not explained by any of the above. Sub-seismic resolution faulting (Walsh *et al.* 1991) may account for up to 40% of the ‘missing’ extension in the upper crust, but cannot explain the much larger observed differences in stretching and thinning between the upper crust, and that of the whole crust and mantle (Fig. 1e).

## Implications of depth-dependent stretching on hydrocarbon maturation and margin subsidence

The implications of depth-dependent stretching for sediment temperature and hydrocarbon maturation history have been calculated for a pseudo-well extracted from line 2 at a distance of 60 km (Fig. 4) from the western end of the profile. Temperature

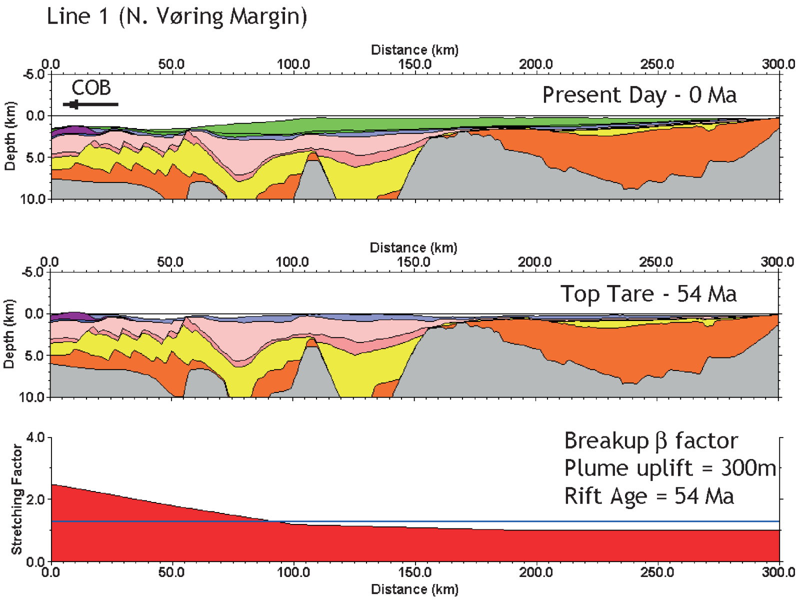


**Fig. 8.** Restored cross sections for line 1 (northern Vøring margin) produced by 2D flexural backstripping and reverse post-rift modelling from present day to top Tare at 54 Ma. Rift age = 54.1 Ma. Lithosphere β factor varies laterally decreasing from β = 2.5 to β = 1 in east. Transient mantle plume uplift for Upper Paleocene is 300 m. Earlier Jurassic–Cretaceous rift at 142 Ma with β = 1.3. $T_e$ = 3 km. The top Tare and top Basalt horizons are restored to sea-level at ~54 Ma consistent with depositional environments.

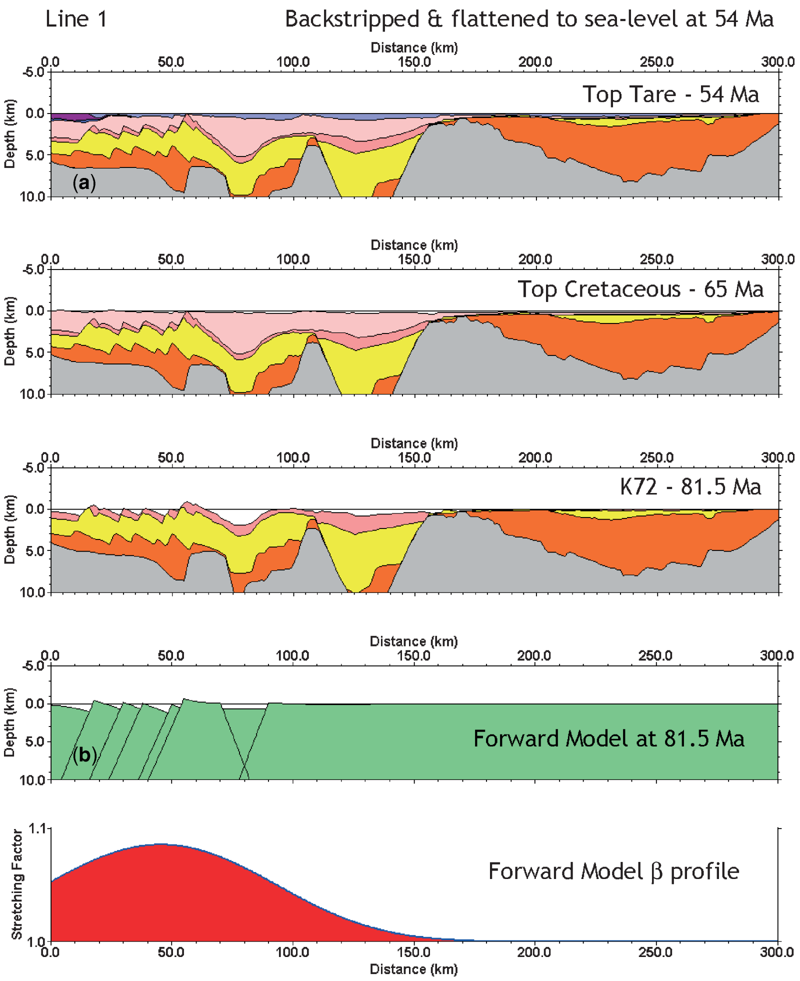


**Fig. 9.** (**a**) Restored cross sections for line 1 (northern Vøring margin) from 54 to 81.5 Ma produced by flexural backstripping and reverse post-rift modelling from section flattened to sea-level at top Tare (54 Ma). β = 1.1 for Late Cretaceous rift with rift age = 81.5 Ma. Earlier Jurassic–Cretaceous rift at 142 Ma with β = 1.3. $T_e$ = 3 km. The restored cross section at 81.5 Ma shows evidence of faulting in the interval 65 to 81.5 Ma. (**b**) 2D syn-rift forward model of Late Cretaceous rifting for line 1. Target structural geometry derived by reverse post-rift modelling to 81.5 Ma. $T_e$ = 3 km. The forward model predicts a maximum β factor of 1.1. Reverse and forward models are consistent at 81.5 Ma.

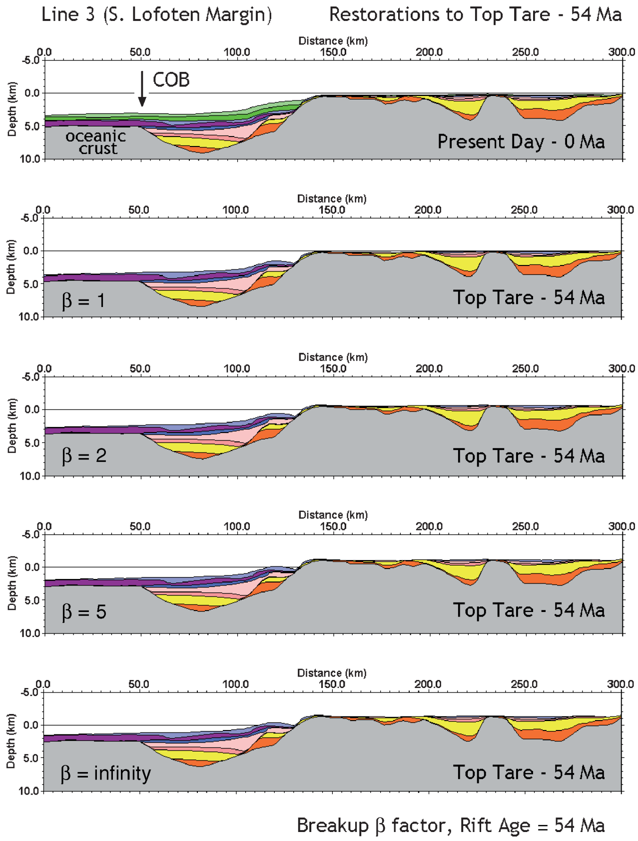


**Fig. 10.** Restored cross sections for line 3 (southern Lofoten margin) from present day to top Tare time (54 Ma) showing sensitivity to lithosphere β factors. Restored cross sections are shown for constant β factors of 1, 2, 5 and infinity. Break-up age is 54.1 Ma. Oceanic crust is located west of $x = 50$ km. A lithosphere β factor of infinity produces 1500 m of palaeobathymetry at break-up at top Tare time (54 Ma). Lithosphere β factors of 1 are required in the east of the section in order to avoid elevating the eastern part of the section above level. Transient mantle plume uplift for Upper Paleocene is 300 m. Earlier Jurassic-Cretaceous rift at 142 Ma with $\beta = 1.3$. $T_e = 3$ km.

evolution has been computed for the burial history recorded in the pseudo-well using a whole lithosphere thermal model. The thermal model includes: sediments, crustal basement and lithospheric mantle; upper-crustal radiogenic heat productivity; multiple rifting; depth-dependent stretching; magmatic sill intrusion and underplating; sediment compaction during burial; lithology and compaction-dependent sediment conductivity, density and radiogenic heat productivity. Hydrocarbon maturation is represented by vitrinite reflectance (%VR) and is computed using the scheme of Sweeney & Burnham (1990).

The influence of depth-dependent stretching on top basement heatflow and maturation (%VR) is shown in Figure 12. Top basement heatflow is plotted against time, while present-day %VR is plotted against depth. The thermal model also includes an earlier rift event at 142 Ma corresponding to the Late Jurassic–Early Cretaceous rift. Figure 12a and d compares the consequences of using depth-uniform lithosphere $\beta = 1$ and 3 to predict heat flow and %VR with those of using depth-dependent stretching consisting of $\beta = 1$ in the upper crust and $\beta = 3$ in the lower crust and mantle. A uniform lithosphere $\beta = 1$ (i.e. no lithosphere extension) for rifting at 54 Ma might be indicated by the absence of any significant Paleocene or Late Cretaceous upper-crustal faulting. In contrast a uniform β stretching-factor = 3 at 54 Ma might be indicated from post break-up thermal subsidence analysis alone. Increasing the lithosphere β factor from 1 to 3 increases both the top basement heat flow and %VR as expected. The effect of using depth-dependent stretching at 54 Ma is to increase top basement heatflow and %VR with respect to the uniform $\beta = 1$ model, but to reduce them with respect to the model with uniform $\beta = 3$. Using a uniform β factor corresponding to that of the upper crust may lead to a substantial underestimate of heat flow and %VR. However, omitting depth-dependent stretching and using a uniform β factor as derived from thermal subsidence analysis may lead to a serious overestimate of heatflow and %VR. The lithosphere thermal model used to predictions heat flow and %VR in Figure 12a and d, uses no radiogenic heat productivity in the upper continental crust. The corresponding heat flow and %VR predicted by a lithosphere thermal model with average continental crust radiogenic heat productivity are shown in Figure 12b and e, and are increased with respect to those of the zero upper-crustal radiogenic heat productivity model.

In Figure 12c and f the effect on top basement heatflow and %VR of a 5 km thick magmatic body (an intrusive sill) emplaced at 15 km depth is shown with and without depth-dependent stretching. The depth-dependent stretching in this case has a $\beta = 1$ the upper crust and $\beta = 3$ for the lower crust and lithospheric mantle. Depth-dependent stretching has a much greater influence on top basement heatflow and %VR. The thermal pulse associated with depth-dependent stretching in this case is both larger in magnitude and duration than that of the magmatic intrusion. Failure to include depth-dependent stretching may have serious consequences on maturation estimates.

Depth-dependent stretching also has an important control on the subsidence history of a continental margin. A schematic summary of the stretching history of the northern Vøring continental margin is shown in Figure 13a. A relatively small magnitude of pre-break-up, depth uniform, Late Cretaceous and Paleocene continental lithosphere stretching precedes a much larger depth-dependent stretching event at continental break-up time (54 Ma). Depth-dependent stretching produces much less thinning of the upper crust than in the lower crust and lithospheric mantle compared with the depth-uniform stretching model. As a consequence, compared with the subsidence history predicted by the depth-uniform lithosphere stretching model (McKenzie 1978), when depth-dependent stretching occurs the initial subsidence $S_i$ is reduced as syn-rift crustal thinning subsidence is lessened with respect to syn-rift thermal uplift (Fig. 13b). When depth-dependent stretching of continental lithosphere occurs at a margin, syn-break-up subsidence may be reduced so that either very little or no syn-break-up subsidence occurs, or even syn-break-up uplift takes place.

The water loaded subsidence predicted by a 1D model of depth-dependent stretching of continental lithosphere is shown in Figure 14a. Subsidence evolution with time is shown for depth-dependent stretching where the lower crust and mantle of margin lithosphere are stretched by $\beta = 3$, while $\beta = 1$ for upper-crustal stretching (i.e. no stretching). Results are compared with the predictions of a uniform stretching model where whole lithosphere $\beta = 1$ and 3. The model also includes earlier depth-uniform stretching events of $\beta = 1.3$ and 1.1 at 142 and 81 Ma, corresponding to Late Jurassic–Early Cretaceous and Late Cretaceous rifting events. The corresponding evolution of continental crustal basement thickness is shown in Figure 14b. It can be seen (Fig. 14a) that the consequence of depth-dependent stretching at break-up at 54 Ma is to give little syn-break-up subsidence compared with the equivalent depth-uniform stretching model. The post-break-up thermal subsidence is however similar. The process of depth-dependent stretching may explain the low palaeobathymetries observed during continental break-up on much of the Norwegian rifted margin.

## A new model for the formation of rifted continental margins

The existence of broad domains, up to 150 km wide, of exhumed mantle between the rotated fault blocks of the thinned continental

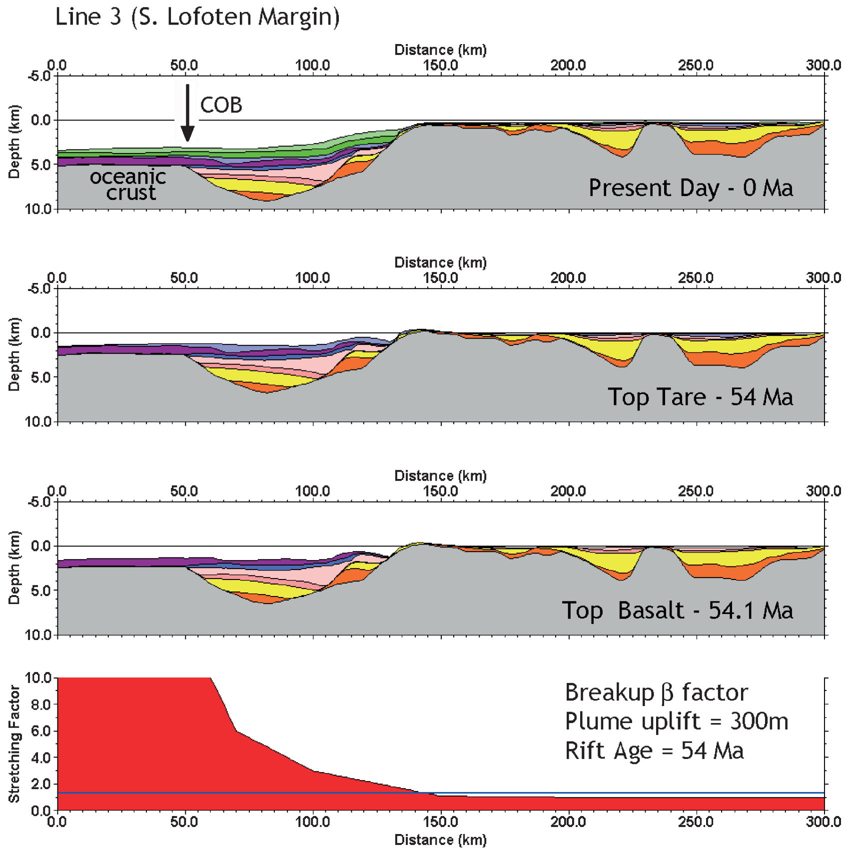


**Fig. 11.** Restored cross sections for line 3 (southern Lofoten margin) produced by 2D flexural backstripping and reverse post-rift modelling from present day to top Tare at 54 Ma and top Basalt at 54.1 Ma. Break-up age = 54.1 Ma. β factor varies laterally decreasing eastwards from β = infinity for oceanic lithosphere to β = 1 in east. Transient mantle plume uplift for Upper Paleocene is 300 m. Earlier Jurassic–Cretaceous rift at 142 Ma with β = 1.3. $T_e$ = 3 km. The top Tare horizon to the west of $x$ = 130 km does not restore to sea level at 54 Ma.

crust and unequivocal oceanic crust, has been observed at non-volcanic margins (Pickup *et al*. 1996; Whitmarsh *et al*. 2001; Manatschal & Nievergelt 1997; Manatschal & Bernoulli 1999). Evidence includes direct sampling on the Iberian (and Grand Banks) margin where mantle rocks (peridotite, lherzolite, harzbergite, dunite) are found immediately beneath post-break-up sediments. Geochemical analysis suggests that the exhumed mantle at non-volcanic margins has a continental geochemistry (Manatschal & Nievergelt 1997; Manatschal & Bernoulli 1999). The existence of exhumed mantle at non-volcanic margins is also indicated by refraction seismology which indicates the absence of a $P_n$ Moho refractor (Pickup *et al*. 1996; Minshull *et al*. 1998), magnetic anomaly data which shows the ocean crust to be absent or extremely thin, and the stratigraphic evidence for exhumed mantle (with continental geochemistry) at the sea bed in the Tethyan Ocean rifted margin of the European Alps (Manatschal & Nievergelt 1997; Manatschal & Bernoulli 1999). The observation of mantle exhumation at non-volcanic margins may explain the historical difficulty of identifying the precise location of the continent–ocean boundary at these margins.

Neither depth-dependent stretching, which is observed at both volcanic and non-volcanic margins, nor mantle exhumation at non-volcanic margins are explained by existing models of rifted margin formation. Many rifted margin models (LePichon & Sibuet, 1981) assume a similar process to that which forms intra-continental rift basins (McKenzie 1978), but with the continental lithosphere stretched by an infinite β factor to form a rifted margin. Such models, however, do not predict or explain depth-dependent stretching or mantle exhumation. New qualitative and quantitative models of rifted margin are required.

The Lofoten and Vøring rifted margin lithosphere subsidence and upper-crustal fault extension study described in this paper suggests that depth-dependent stretching occurs during sea-floor spreading initiation or early seafloor spreading rather than during pre-break-up rifting. A new model of rifted margin formation is proposed that assumes that the dominant process for thinning rifted continental margin lithosphere is seafloor spreading initiation, rather than pre-break-up intra-continental rifting. Observations (Davis & Kusznir 2004) suggest that upper-crustal β factors for pre-break-up lithosphere stretching are relatively small and less than 1.5. In the case of the Lofoten and Vøring margins, pre-break-up β factors are less than 1.1 for Paleocene and Late Cretaceous stretching.

In the pre-break-up intra-continental rifting phase (Fig. 15a), extensional faulting in the upper crust is balanced by distributed plastic deformation in the lower crust and mantle (McKenzie 1978). Pre-break-up stretching of the upper continental crust by faulting with small β(< 1.5) gives way first to localized dyke intrusion, and pure shear stretching of the deeper continental lithosphere evolves into a divergent upwelling flow within continental lithosphere similar in geometry to that found at ocean ridges (Fig. 15b). This rapidly leads to thinning of continental lithosphere, the start of seafloor spreading and the formation of oceanic crust (Fig. 15c).

Divergent mantle flow models have been successfully applied to ocean ridges (Buck, 1991; Spieglemann and McKenzie, 1987; Spieglemann and Reynolds, 1999). The strategy for modelling rifted continental margins is to model both the effects of pre-break-up lithosphere stretching and of seafloor spreading initiation. Simple fluid-flow models of ocean ridge processes, using analytical iso-viscous corner-flow solutions (Batchelor 1967), show that the divergent motion of upwelling mantle beneath ocean ridges produces depth-dependent stretching. Single-phase fluid-flow models are being developed to model the initiation of seafloor

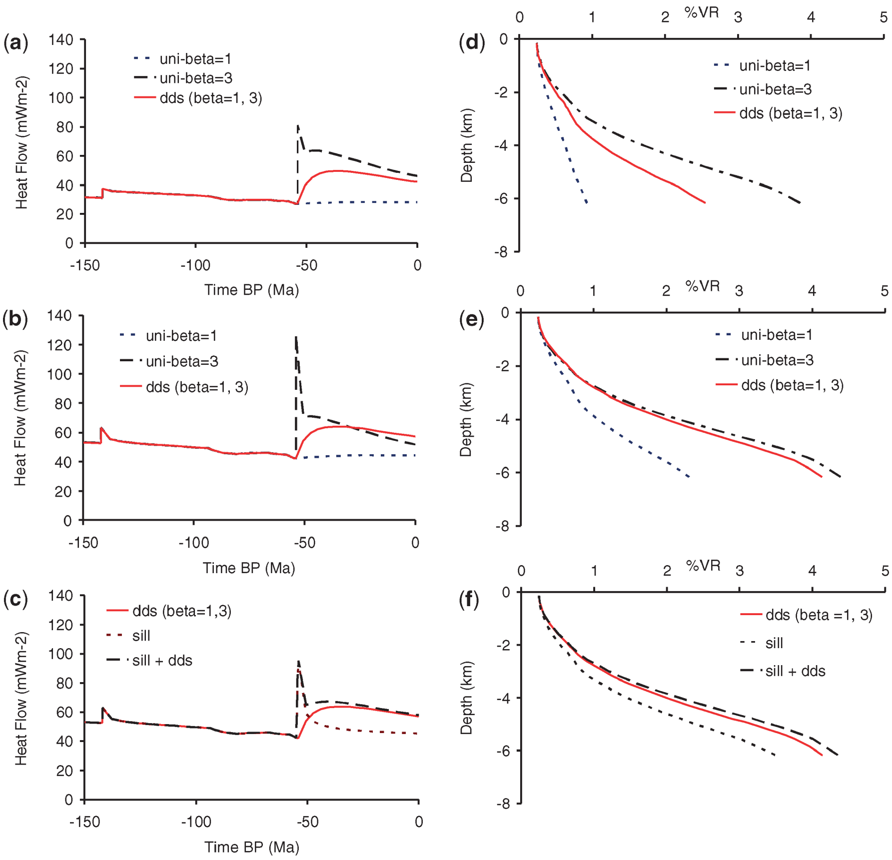


**Fig. 12.** Top basement heat flow and maturation (%VR) are dependent on depth-dependent stretching within continental margin lithosphere. (**a**) Predicted top basement heatflow with time and (**d**) present day %VR with depth compared for depth-dependent stretching with $\beta = 1$ in the upper crust and $\beta = 3$ in the lower crust and mantle, and predictions using depth uniform lithosphere stretching with $\beta = 1$ and 3. Failure to include depth-dependent stretching may lead to a substantial underestimate of top basement heatflow and %VR. The thermal model is dynamic and includes compacting sediments, continental crust and lithospheric mantle. Burial history is for a pseudo-well located on line 3 (southern Lofoten margin) at $x = 60$ km. An earlier depth-uniform rift event at 142 Ma is included in the model. (**b**,**e**) Top basement heat flow and %VR predicted as in (**a**,**d**) but including average upper continental crust radiogenic heat productivity in lithosphere thermal model. (**c**,**f**) Comparison of effects of 5 km thick sill intruded at 15 km depth and depth-dependent stretching with $\beta = 1$ in the upper crust and $\beta = 3$ in the lower crust and mantle on heat flow history and %VR with depth. Depth-dependent stretching flow may increase top basement heatflow in magnitude and duration more than magmatic intrusions, and may also have a greater effect on %VR.

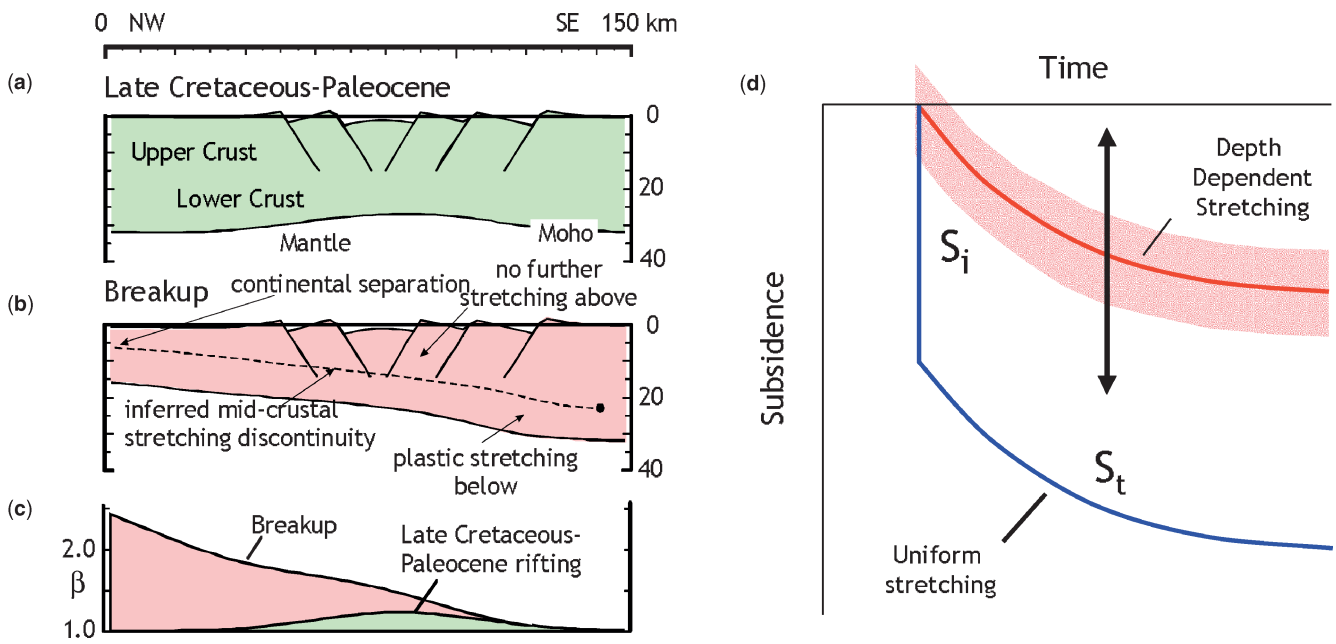


**Fig. 13.** (**a**–**c**) Schematic summary of the stretching history of the northern Vøring continental margin showing small magnitude depth uniform pre-break-up continental lithosphere stretching in Late Cretaceous and Paleocene preceding much larger magnitude depth-dependent lithosphere stretching at break-up. (**d**) Depth-dependent stretching has an important control on subsidence history and leads to a reduction of initial subsidence ($S_i$) compared with depth uniform lithosphere stretching (cf. McKenzie 1978) resulting in low syn-break-up bathymetry or even emergence.

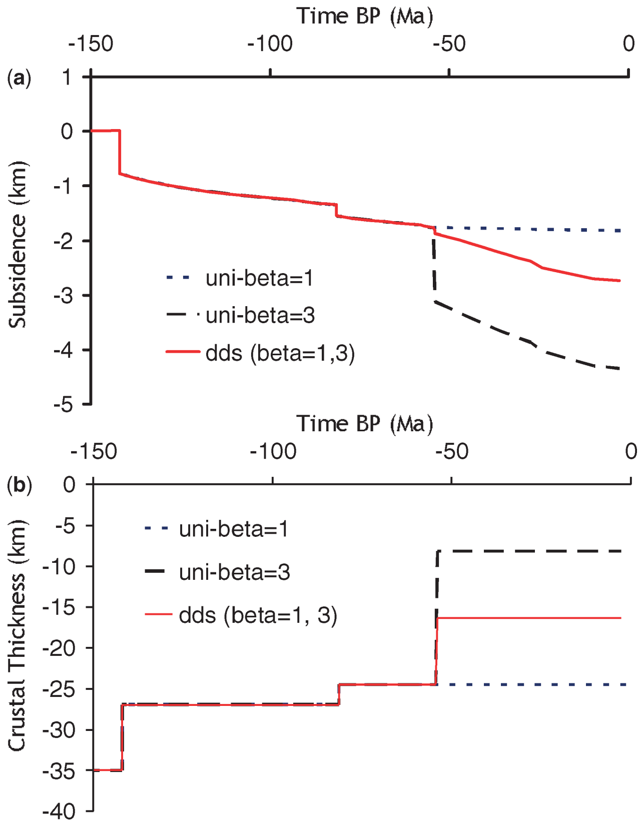


**Fig. 14.** (**a**) Sensitivity of rifted margin water-loaded subsidence history to lithosphere depth-dependent stretching predicted by 1D model. Earlier depth uniform lithosphere stretching at 142 and 81 Ma with $\beta = 1.3$ and 1.1 respectively. Break-up age = 54 Ma. Depth-dependent stretching at 54 Ma with $\beta = 1$ for upper crust and $\beta = 3$ for lower crust and mantle generates little syn-break-up subsidence compared with depth-uniform $\beta = 3$. (**b**) Corresponding crustal thickness history.

spreading, and the stretching and thinning of the young rifted continental margin. Our model formulation uses the Batchelor (1967) stream-function corner-flow solution. Continent lithosphere material is advected to predict lithosphere and crustal thinning. Temperature is predicted by a coupled thermal diffusion and advection solution. The ocean ridge fluid-flow stream-function solution is isoviscous, kinematic (Fig. 15d) and requires the definition of $V_x$ (the half-spreading rate of the oceanridge) and $V_z$ (the upwelling velocity beneath the ridge-axis). Mantle convection modelling (Nielsen & Hopper 2002) suggests that for volcanic margins $V_z/V_x$ may be $>5$ during seafloor spreading initiation, reducing to $V_z/V_x$ approximately 1 after a few Ma, while for non-volcanic margins, lower values of $V_z/V_x$ (of the order of 1) are expected during seafloor spreading initiation.

Application of the new model of seafloor spreading initiation to rifted margin formation is shown in Figure 16 for both ‘passive’ and ‘active’ rifted margin formation, with and without pre-break-up pure-shear lithosphere stretching. Model results are shown after 10 Ma of seafloor spreading with $V_x = 2$ cm/year. The ‘passive’ model has $V_z = 3$ cm/year at all times, while the ‘active’ model has $V_z = 10$ cm/year for time $<2$ Ma and $V_z = 3$ cm/year for time $>2$ Ma. Model solutions are also shown which include pre-break-up pure-shear lithosphere stretching with 50 km of pre-break-up extension distributed over a width of 300 km, giving a maximum β value of 1.5. All models shown in Figure 16 show depth-dependent stretching. The models for which $V_z$ is approximately equal to $V_x$, corresponding to ‘passive’ rifting, show an oceanward flow of the continental mantle leading to mantle exhumation (Fig. 16a and b). In contrast, the models for which $V_z \gg V_x$, corresponding to ‘active’ rifting, show transport of the continental mantle towards the continent (Fig. 16c and d). The effects of the

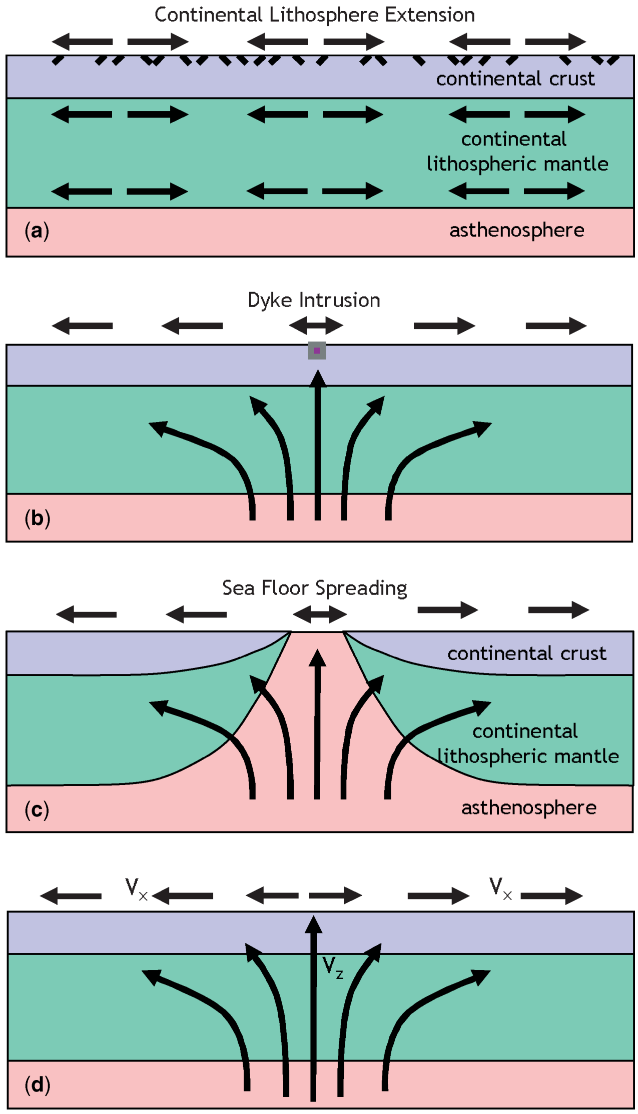


**Fig. 15.** (**a**) Pre-break-up continental rifting with upper-crustal faulting balanced at depth in the lower crust and lithospheric mantle by pure shear (plastic) deformation for small $\beta(<1.5)$. (**b**) Upper crustal extension by faulting is replaced by dyke injection, and at depth pure shear extension of continental lithosphere gives way to divergent upwelling of continental lithosphere and asthenosphere generating depth-dependent stretching and thinning, leading to sea-floor spreading initiation. (**c**) Sea-floor spreading commences and the divergent upwelling flow of mantle material continues to generate depth-dependent stretching of continental lithosphere. (**d**) Illustration of the seafloor spreading initiation model. The divergent upwelling mantle-flow of the initiating ocean-ridge is predicted using the Batchelor (1967) stream-function corner-flow solution. The stream-function solution is isoviscous and requires the definition of $V_x$ (half spreading rate of ocean-ridge) and $V_z$ (upwelling velocity beneath ocean-ridge ridge-axis). Continental lithosphere material is advected to predict lithosphere and crustal thinning. Temperature is predicted by a coupled thermal diffusion and advection solution.

pre-break-up pure-shear lithosphere stretching can be seen (cf. Fig. 16a and c with Fig. 16b and d). However, the effects of 50 km of pure shear lithosphere extension are minor compared with that of seafloor spreading initiation.

An application of the model to a volcanic margin is shown in Figure 17. Model parameters are: elapsed time since sea-floor spreading initiation = 10 Ma; $V_x = 2$ cm/year; $V_z = 10$ cm/year for $t < 2$ Ma; $V_z = 3$ cm/year for $t > 2$ Ma; and pre-break-up stretching $\beta = 1.5$ distributed over a pure shear width of 300 km. Flow streamlines and velocity history ($V_x$ and $V_z$) are shown in Figures 17a, b and e. The thinning of continental margin lithosphere

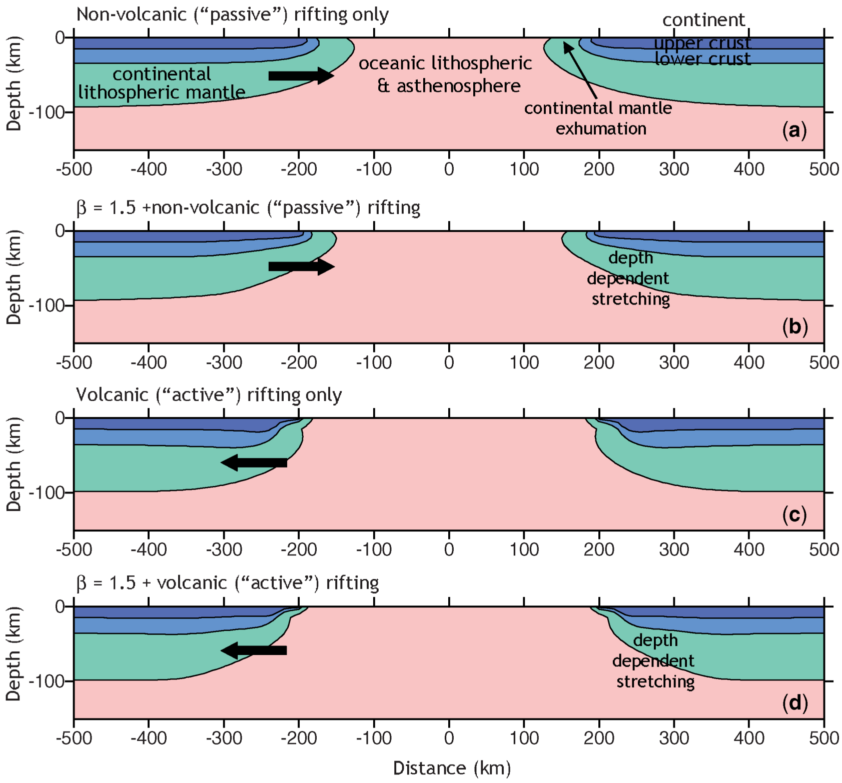


**Fig. 16.** Application of the sea-floor spreading initiation model to 'passive' and 'active' rifted margin formation without and with pre-break-up pure-shear lithosphere stretching. Time elapsed is 10 Ma. (**a**) 'passive' rifting with $V_x = 2$ cm/year and $V_z = 3$ cm/year, (**b**) 'passive' rifting and pre-break-up β factor = 1.5, (**c**) 'active' rifting with $V_x = 2$ cm/year, $V_z = 10$ cm/year for time $<2$ Ma and $V_z = 3$ cm/year for time $>2$ Ma, (**d**) 'active' rifting and pre-break-up β factor = 1.5.

and lithosphere temperature structure is shown in Figures 17c and d. The model predicts depth-dependent stretching, margin subsidence and heat flow (Fig. 17f, g and h). The distribution and sense of depth-dependent stretching is qualitatively similar to that observed on the Lofoten margin.

Driscoll & Karner (1998) noted that the sense of depth-dependent stretching, in which stretching of the upper crust is much less than that of the whole crust and lithospheric mantle, is consistent with an upper plate location within a lithosphere simple shear extension model (Wernicke 1985; Lister *et al.* 1991), and that all rifted margins, including conjugate margins, appear to be upper plate. Driscoll & Karner (1998) named this the 'Upper Plate Paradox'. The model described above and illustrated in Figures 16 and 17 predicts symmetric depth-dependent stretching from seafloor spreading initiation and gives 'upper plate' behaviour on both conjugate rifted margins, providing an explanation for the 'Upper Plate Paradox'.

The volcanic margin model shown in Figure 17 uses $V_z \gg V_x$. For the volcanic margin, depth-dependent stretching is achieved by ocean ridge mantle flow pushing the continental lower crust and lithospheric mantle towards the continent. For a non-volcanic margin, $V_z$ is similar in magnitude to $V_x$ (Nielsen & Hopper 2002). A model with $V_z$ approximately equal to $V_x$, appropriate for non-volcanic margins, also produces depth-dependent stretching but by generating an oceanward flow of the continental lower crust and lithospheric mantle leading to the exhumation of a broad region of continental mantle.

## Summary

Tertiary subsidence patterns along the outer part of the Lofoten, Vøring and Møre segments of the Norwegian rifted continental margin require depth-dependent stretching of lithosphere at continental break-up. The southern Lofoten and northern Vøring margins show only a small magnitude of lithosphere extension by faulting (β < 1.1) preceding break-up in the Paleocene and latest Late Cretaceous. In contrast large lithosphere β factors (>2.5) are required at 54 Ma to restore top Tare and top Basalt to sub-aerial depositional environments. The absence of significant Paleocene extensional faulting on the Lofoten and Vøring margins may be explained by depth-dependent stretching occurring during sea-floor spreading initiation rather than during pre-break-up intra-continental rifting.

Depth-dependent stretching has an important effect on temperature and %VR evolution in depth and time. Failure to include the large β factors for the lower crust and lithospheric mantle leads to a serious under-prediction of sediment temperature and hydrocarbon maturation. Depth-dependent stretching may have a stronger influence on temperature and maturation than magmatic underplating.

New discoveries of depth-dependent stretching and mantle exhumation at rifted margins require new models of rifted margin formation. Observations suggest that the dominant process responsible for thinning continental margin lithosphere is seafloor spreading initiation. A new model of seafloor spreading initiation and rifted margin formation has been developed. The new model uses a single-phase fluid-flow model of divergent ocean-ridge mantle flow to predict continental margin lithosphere thinning and thermal evolution during seafloor spreading initiation. The new model may be used to predict depth-dependent stretching, and margin subsidence and heat flow history.

We thank ConocoPhillips for allowing us to publish the work described in this paper, Elizabeth Eide and Filoppos Tsikalas for providing the maps shown in Figure 2, P. van Veen for providing stratigraphic data, and C. Berndt, M. Davis, M. Cheadle, N. Driscoll, G. Karner, E. Lundin, T. Minshull and R. Whitmarsh for helpful and stimulating discussions.

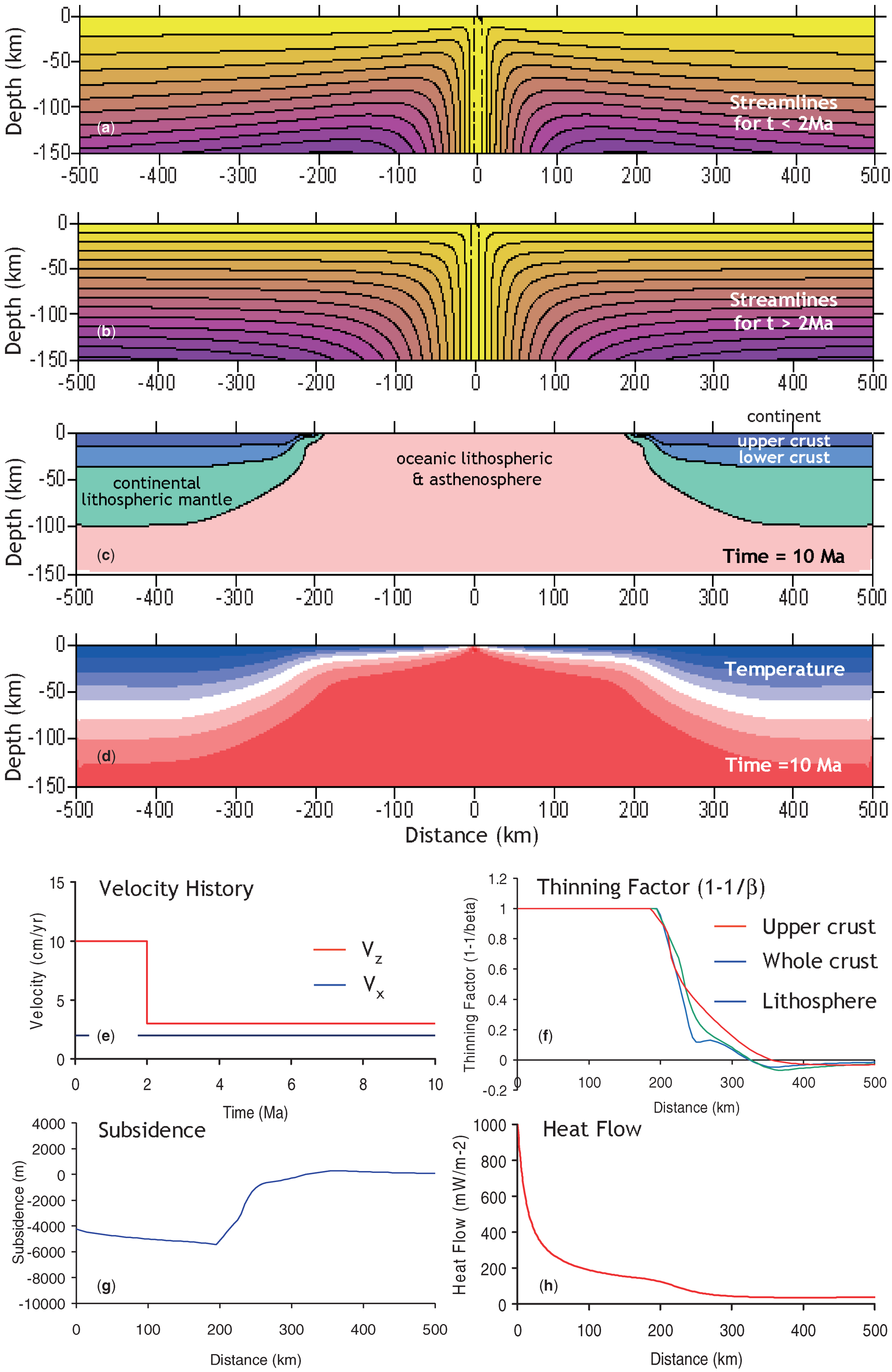


**Fig. 17.** Application of the ocean ridge initiation model to a volcanic rifted margin. Time elapsed since seafloor spreading initiation is 10 Ma. (**a**,**b**) ocean-ridge flow stream lines, (**c**) predicted thinning of the rifted continental margin lithosphere, (**d**) predicted lithosphere temperature, (**e**) $V_x$ and $V_z$ history (kinematic input parameters), profiles of (**f**) predicted thinning-factors (1-1/β) for upper crust, whole crust and whole lithosphere showing depth-dependent stretching, (**g**) margin subsidence (and uplift), and (**h**) top basement heat flow.

We also thank F. Tsikalas and S. Price for their reviews and constructive comments. The development and testing of new rifted margin formation models forms part of the iSIMM (integrated Seismic Imaging and Modelling of Margins) project. The iSIMM project is supported by funding from NERC, DTI, Agip, BP, Amerada Hess, Anadarko, Conoco, Phillips, Shell, Statoil and WesternGeco.

## References

Batchelor, G. K. 1967. *An Introduction to Fluid Dynamics*. Cambridge University Press.

Baxter, K., Cooper, G. T., Hill, K. C. & O'Brian, G. W. 1999. Late Jurassic subsidence and passive margin evolution in the Vulcan Sub-basin, north-west Australia: constraints from basin modelling. *Basin Research*, **11**, 97–111.

Berggren, W. A., Kent, D. V., Swisher, C. C. III & Aubrry, M. P. 1995. A revised Cenozoic geochronology and chronostratigraphy. *In*: Berggren, W. A., Kent, D. V., Swisher, C. C. III & Hardenol, J. III (eds) *Geochronology, Time Scales and Global Stratigraphic Correlation*, Society for Sedimentary Geology (SEPM) Special Publication, **54**, 129–212.

Berndt, C., Planke, S., Alvestad, E., Tsikalas, F. & Rasmussen, T. 2001. Seismic volcanostratigraphy of the Norwegian margin: constarints on break-up process. *Journal of the Geological Society, London*, **158**, 413–426 .

Blystad, P., Brekke, H., Færseth, R. B., Larsen, B. T., Skogseid, J. & Tørudbekken, B. 1995. Structural elements of the Norwegian continental shelf. Part II: the Norwegian Sea Region. *Norwegian Petroleum Directorate Bulletin*, **8**, 45.

Brekke, H. 2000. The tectonic evolution of the Norwegian Sea continental margin with emphasis on the Vøring and Møre Basins. *In*: Nøttvedt, A. *et al.* (eds) *Dynamics of the Norwegian Margin*. Geological Society, London, Special Publications, **167**, 327–378.

Buck, W. R. 1991. Modes of continental lithospheric extension. *Journal of Geophysical Research*, **96**, 20161–20178.

Cande, S. C. & Kent, D. V. 1992. A new geomagnetic timescale for the Late Cretaceous and Cenozoic. *Journal of Geophysical Research*, **97**, 13917–13951.

Caston, V. N. D. 1976. Tertiary sediments of the Vøring Plateau, Norwegian Sea, recovered by Leg 38 of the Deep Sea Drilling Project. *In*: Talwani, M. & Udintsev, G. *et al.* (eds) *Initial Reports of the Deep Sea Drilling Project, Volume 38*. U.S. Government Printing Office, Washington, 1101–1168.

Dalland, A., Worsley, W. & Ofstad, K. 1988. A lithostratigraphic scheme for the Mesozoic and Cenozoic succession offshore mid- and northern Norway. *Norwegian Petroleum Directorate, Bulletin*, **4**, 65.

Davis, M. & Kusznir, N. J. 2004. Depth-dependent lithospheric stretching at rifted continental margins. *In*: Karner, G. D. (ed.) *Proceedings of NSF Rifted Margins Theoretical Institute*. Columbia University Press, 92–136.

Doré, A. G. 1991. The structural foundation and evolution of Mesozoic seaways between Europe and the Arctic. *Palaeogeography, Palaeoclimatology and Palaeoceanography*, **87**, 441–446.

Doré, A. G., Lundin, E. R., Jensen, L. N., Birkeland, O., Eliassen, P. E. & Fichler, C. 1999. Principal tectonic events in the evolution of the northwest European Atlantic margin. *In*: Fleet, A. J. & Boldy, S. A. R. (eds) *Petroleum Geology of Northwest Europe: Proceedings of the 5th Conference*. Geological Society, London, 41–61.

Driscoll, N. & Karner, G. 1998. Lower crustal extension across the Northern Carnarvon basin, Australia: Evidence for an eastward dipping detachment. *Journal of Geophysical Research*, **103**, 4975–4991.

Eide, E. E. 2002. *BATLAS – Mid-Norway Plate Reconstruction Atlas with Global and Atlantic Perspectives*. Geological Survey of Norway.

Eldholm, O., Thiede, J., Taylor, E. 1989. Evolution of the Vøring volcanic margin. *In*: Eldholm, O., Thiede, J. & Taylor, E. *et al.* (eds) *Proceedings of the Ocean Drilling Program, Scientific Results,* **104**. Ocean Drilling Program, College Station, TX, 1033–1065.

Eldholm, O., Skogseid, J., Planke, S. & Gladczenko, T. P. 1995. Volcanic margin concepts. *In*: Banda, E. (ed.) *Rifted Ocean-Continent Boundaries*. Kluwer, Dordrecht, 1–16.

Kusznir, N. J. & Ziegler, P. A. 1992. The mechanics of continental extension and sedimentary basin formation – a simple-shear pure-shear flexural cantilever model. *Tectonophysics*, **215**, 117–131.

Kusznir, N. J., Marsden, G. & Egan, S. S. 1991. A flexural-cantilever simple-shear/pure-shear model of continental lithosphere extension: applications to the Jeanne D'Arc basin, Grand banks and Viking Graben North Sea. *In*: Roberts, A. M., Yielding, G. & Freeman, B. (eds) *Geometry of Normal Faults*. Geological Society, London, Special Publications, **56**, 41–60.

Kusznir, N. J., Roberts, A. M. & Morley, C. 1994. Forward and reverse modelling of rift basin formation. *In*: Lambiase, J. (ed.) *Hydrocarbon Habitat in Rift Basins*. Geological Society, London, Special Publications, **80**, 33–56.

Kusznir, N. J., Hunsdale, R. & Roberts, A. M. 2004. Timing of depth-dependent lithosphere stretching on the S. Lofoten rifted margin offshore Mid-Norway: Pre-breakup or post-breakup? *Basin Research*, **16**, 279–296.

Le Pichon, X. & Sibuet, J. C. 1981. Passive margins: a model of formation. *Journal of Geophysical Research*, **86**, 3708–3720.

Lister, G. S., Etheridge, M. A. & Symonds, P. A. 1991. Detachment models for the formation of passive continental margins. *Tectonics*, **10**, 1038–1064.

Lundin, E. R. & Doré, A. G. 1997. A tectonic model for the Norwegian passive margin with implications for the NE Atlantic Early Cretaceous to break-up. *Journal of the Geological Society, London*, **154**, 545–550.

Manatschal, G. & Bernoulli, D. 1999. Architecture and tectonic evolution of nonvolcanic margins: Present day Galicia and ancient Adria. *Tectonics*, **18**, 1099–1119.

Manatschal, G. & Nievergelt, P. 1997. A continent–ocean transition recorded in the Err and Platta nappes (Eastern Switzerland). *Eclogae Geologicae Helvetiae*, **90**, 3–27.

McKenzie, D. P. 1978. Some remarks on the development of sedimentary basins. *Earth and Planetary Science Letters*, **40**, 25–32.

Minshull, T. A., Dean, S. M., White, R. S. & Whitmarsh, R. B. 1998. Restricted melting at the onset of seafloor spreading: ocean-continent transition zones at non-volcanic rifted margins. *Transactions of the American Geophysical Union*, **79**, 906.

Mjelde, R., Sellevoll, M. A., Shimamura, H., Iwasaki, T. & Kanazawa, T. 1993. Crustal structure beneath Lofoten, N. Norway, from vertical incidence and wide-angle seismic data. *Geophysical Journal International*, **114**, 116–126.

Mjelde, R., Digranes, P., Shimamura, H., Shiobara, H., Kodira, S., Brekke, H., Egebjerg, T., Sørnes, N. & Thorbjørnsen, S. 1998. Crustal structure of the northern part of the Vøring Basin, mid-Norway margin, from wide-angle seismic and gravity data. *Tectonophysics*, **293**, 175–205.

Mosar, J., Torsvik, T. H. & The BAT team, T. H. 2002. Opening the Norwegian and Greenland Seas: Plate tectonics in Mid Norway since the Late Permian. *In*: Eide, E. E. (ed.) *BATLAS – Mid Norway plate reconstruction atlas with global and Atlantic perspectives*, Geological Survey of Norway, 48–59.

Nadin, P. A. & Kusznir, N. J. 1995. Paleocene uplift and Eocene subsidence in the northern North Atlantic from 2D forward and reverse stratigraphic modelling. *Journal of the Geological Society*, **152**, 833–848.

Nadin, P., Kusznir, N. J. & Cheadle, M. J. 1997. Early Tertiary plume uplift in the North Sea and Faeroe-Shetland Basin. *Earth and Planetary Science Letters*, **148**, 109–127.

Nielsen, T. K. & Hopper, J. R. 2002. Formation of volcanic rifted margins: Are temperature anomalies required? *Geophysical Research Letters*, **29**, 2022–2025.

Pickup, S. L. B., Whitmarsh, R. B., Fowler, C. M. R. & Reston, T. J. 1996. Insight into the nature of the ocean-continent transition off West Iberia from a deep multichannel seismic reflection profile. *Geology*, **24**, 1079–1082.

Planke, S., Symonds, P., Alvestad, E. & Skogseid, J. 2000. Seismic volcano-stratigraphy of large-volume basalt extrusive complexes on rifted margins. *Journal of Geophysical Research*, **105**, 19335–19351.

Ren, S., Faleide, J. I., Eldholdm, O., Skogseid, J. & Gradstein, F. 2003. Late Cretaceous–Paleocene tectonic development of the NW Vøring Basin. *Marine and Petroleum Geology*, **20**, 177–206.

Roberts, A. M., Lundin, E. R. & Kusznir, N. J. 1997. Subsidence of the Vøring Basin and the influence of the Atlantic continental margin. *Journal of the Geological Society London*, **154**, 551–557.

Roberts, A. M., Kusznir, N. J., Yielding, G. & Styles, P. 1998. Backstripping extensional basins: the need for a sideways glance. *Petroleum Geoscience*, **4**, 327–338.

Roberts, D. G., Thompson, M., Mitchener, B., Hossack, J., Carmichael, S. M. M. & Bjornseth, H. M. 1999. Palaeozoic to Tertiary rift and basin dynamics; mid-Norway to the Bay of Biscay; a new context for hydrocarbon prospectivity in the deep water frontier. *In*: Fleet, A. J. & Boldy, S. A. R. (eds) *Petroleum Geology of Northwest Europe: Proceedings of the 5th Conference*. Geological Society, London, 7–40.

Sigmond, E. M. O. 2002. *Geological map, Land and Sea Areas of Northern Europe*. Geological Survey of Norway, Scale 1:3 Million.

Skogseid, J., Planke, S., Faleide, J. I., Pedersen, T., Eldholm, O., Neverdal, F. 2000. NE Atlantic continental rifting and volcanic margin formation. *In*: Nottvedt, A. *et al.* (eds) *Dynamics of the Norwegian Margin*. Geological Society, London, Special Publications, **167**, 295–326.

Spieglemann, N. & McKenzie, D. 1987. Simple 2-D models for melt extraction at mid-ocean ridges and island arcs. *Earth and Planetary Science Letters*, **83**, 137–152.

Spieglemann, M. & Reynolds, J. R. 1999. Combined dynamic and geochemical evidence for convergent melt flow beneath the East Pacific Rise. *Nature*, **402**, 282–285.

Sweeney, J. J. & Burnham, A. K. 1990. Evaluation of a simple model of vitrinite reflectance based on chemical kinetics. *AAPG Bulletin*, **74**, 1559–1570.

Talwani, M. & Eldholm, O. 1972. Continental Margin off Norway; A Geophysical Study. *Geological Society of America Bulletin*, **83**, 3575–3606.

Talwani, M. & Eldholm, O. 1977. Evolution of the Norwegian-Greenland Sea. *Geological Society of America Bulletin*, **88**, 969–999.

Tsikalas, F., Faleide, J. I. & Eldholm, O. 2001. Lateral variations in tectono-magmatic style along the Lofoten-Vesteralen volcanic margin off Norway. *Marine and Petroleum Geology*, **18**, 807–832.

Tsikalas, F., Eldholm, O. & Faleide, J. I. 2002. Early Eocene sea floor spreading and continent-ocean boundary between Jan Mayen and Senja Fracture zones in the Norwegian-Greenland Sea. *Marine Geophysical Research*, **23**, 247–270, 807–832.

Walsh, J., Watterson, J. & Yielding, G. 1991. The importance of small-scale faulting in regional extension. *Nature*, **351**, 391–393.

Wernicke, B. 1985. Uniform-sense simple shear of the continental lithosphere. *Canadian Journal of Earth Sciences*, **22**, 108–125.

White, R. & McKenzie, D. 1989. Magmatism at rift zones: the generation of volcanic continental margins and flood basalts. *Journal of Geophysical Research*, **94**, 7685–7729.

White, R. S. & McKenzie, D. 1995. Mantle plumes and flood basalts. *Journal of Geophysical Research*, **100**, 17543–17585.

Whitmarsh, R. B., Manatschal, G. & Minshull, T. A. 2001. Evolution of magma-poor continental margins from rifting to sea-floor spreading. *Nature*, **413**, 150–153.